



TECHNICAL NOTES

NATIONAL ADVISORY COMMITTEE FOR AERONAUTICS.

Reid, E. G.

No. 209

TESTS OF ROTATING CYLINDERS.

By Elliott G. Reid,
Langley Memorial Aeronautical Laboratory.

FILE COPY

To be returned to
the files of the Langley
Memorial Aeronautical
Laboratory

December, 1924.

NATIONAL ADVISORY COMMITTEE FOR AERONAUTICS.

TECHNICAL NOTE NO. 209.

TESTS OF ROTATING CYLINDERS.

By Elliott G. Reid.

Summary

Tests have been made in the No. 1 (5 ft. atmospheric) wind tunnel at Langley Memorial Aeronautical Laboratory to determine the air forces acting on rotating cylinders with axes perpendicular to the direction of motion. Two cylinders were tested; one had a circular cross-section, the other that of a Greek cross. A compound strut was also tested, the rotating circular cylinder constituting its upstream portion. In the case of the circular cylinder, a lift coefficient of 9.5 was obtained without reaching a maximum; the ratio of lift to drag reached a value of 7.8. Considered as airfoils, the cross cylinder and compound strut were not so efficient. Less power was required to rotate the circular cylinder in moving than in still air.

Introduction

A combination of translation and circulation is the basic concept of the theory of airfoils proposed by Kutta, as well as those of Joukowski, von Mises, Lanchester and Prandtl (Reference 1). The tests described below constitute an attempt to measure the forces arising from controlled combination of these two types of flow.

Methods and Apparatus

All the models were tested in infinite length-diameter ratio; cross-sectional dimensions may be had from Fig. 1. The set-up is diagrammatically shown in Figs. 2 and 3. The cylinder was supported in a large self-aligning ball bearing A, and restrained at its lower end by two pairs of horizontal wires, attached to the ball bearing B, which were respectively parallel and perpendicular to the air flow. An electric motor C, drove the cylinder through the flexible rubber connection D. The balances used to measure drag and cross-wind forces are shown at E and F. Tension in the wire systems was maintained by the counterweights G, G' and elasticity provided by rubber inserts H, H'. Turnbuckles between cylinder and balances (not shown) were used to counteract the elastic deformations of the restraining system under the action of air forces, thus eliminating the pendulum reaction of the cylinder.

The observed data consist of drag and cross-wind forces, airspeed, R.P.M. of the cylinder and electrical input to the motor driving the cylinder. Individual observations were made by bringing airspeed and R.P.M. to the desired values and measuring the other quantities simultaneously.

The program of test was as follows: The circular cylinder was tested at an airspeed of 15 m/s. (49.2 ft./sec.), and increasing rotative speeds until the power limit of the drive motor was reached. The airspeed was then reduced to 10 m/s. (32.8 ft./sec.) and the process repeated. It became necessary to go to 7 (23) and, finally,

5 m/s. (16.4 ft./sec.) in order to reach a maximum "lift/drag" ratio.

The performance of the cross cylinder, at 15 m/s. (49.2 ft./sec.), was very erratic. A marked hysteresis loop made its appearance in the vector diagram of resultant air force and, when excessive vibration was encountered at 3000 R.P.M. and 10 m/s. (32.8 ft./sec.) airspeed, the work on this model was discontinued.

The first test on the compound strut, in which the gap between cylinder and fairing was $1/8$ ", showed this combination to be inferior to the circular cylinder when considered as an airfoil. A large scale effect was also found, coefficients for a fixed ratio of peripheral speed to airspeed varying with the airspeed. Tests with a $3/8$ " gap were made next but such a large increase of drag was found that no further combinations were tried.

After the completion of the force measurements, apparatus was installed to allow the introduction of smoke filaments into the airstream just in front of the cylinder and a series of photographs were taken at various combinations of rotative and airspeeds.

Reduction of Data - Presentation of Results

The air forces acting on the cylinder were assumed to be symmetrical about a horizontal plane through the tunnel axis, i.e., the resultant air force was assumed to act in this plane. The dimensions of the set-up were such that a factor 1.965 had to be applied to the measured forces to give true forces acting on the cylinder. Coefficients were derived on a basis of projected area of

the cylinder as follows:

$$C_D = \frac{D}{qS}$$

$$C_{CW} = \frac{CWF}{qS}$$

$$r = \frac{V'}{V}$$

wherein q is the dynamic pressure, S the projected area of the cylinder, D the drag force, CWF the cross-wind, or "lift" force, V' the peripheral speed and V the airspeed.

The data from tests on the circular cylinder are given in Tables I and II. Fig. 4 is a vector diagram which shows the variations of resultant as well as component forces throughout the range explored, Fig. 5 indicates the variation of cross-wind force with the ratio of peripheral to translational speed, and Fig. 6 shows the power necessary for rotation at zero and 15 m/s (49.2 ft./sec.) airspeed. Corresponding data on the cross cylinder are given in Tables III and IV; Figs. 7, 8 and 9 are the vector diagram, plot of cross-wind force against speed ratio, and power consumption against R.P.M., respectively. The data taken on the compound strut with 1/8" gap, are given in Tables V and VI; Figs. 10, 11 and 12 are plotted therefrom. Results from the second strut combination are given in Table VII and plotted in Figs. 13 and 14.

Discussion

As no mathematical or physical analysis of the results has been attempted, as yet, this discussion will, necessarily, consist

in calling the reader's attention to those points which seem of greatest importance. Let us consider, first, the tests of the circular cylinder.

The sudden appearance of the cross-wind force at $r = 0.5$ seems so definitely established that mere coincidence is doubtful. Unfortunately, no study of the smoke flow was made in this range so it is not known whether there is an abrupt change in the flow pattern to account for the phenomenon.

Beyond the ratio $r = 0.5$, the cross-wind force increases steadily through quite a range in which there is practically no variation in drag, the value of the latter remaining constant between $r = 0.5$ and 2.0 . With values of r greater than 2.0 the drag increases and the maximum ratio of lift to drag (7.8) is attained when $r = 2.5$, approximately. It is noted that the drag coefficient at this point is almost identical with that of the stationary cylinder.

The high values of C_{QW} result, of course, from the very unsymmetric velocity distribution around the cylinder. The smoke photographs (Figs. 15, 16 and 17) clearly depict the gradual distortion of the symmetrical flow pattern with increasing rotation and the building up of a very high velocity region opposite one of considerably reduced velocity. Thus the rotation produces the same sort of velocity distribution as does camber in the case of an airfoil. The greater dissymmetry of this flow, as compared to that about an airfoil, is undoubtedly due to the fact that the

proportionate increase and decrease of the free stream velocity is considerably augmented by the rotation.

In connection with the variation of drag, the following points are noted: The smoke photographs show that at small values of r the groups of streamlines from the two sides of the cylinder do not diverge so markedly as is the case with the motionless cylinder. This accounts for the first reduction of drag. Through the range in which C_D remains constant, although C_{GW} increases rapidly, there must be balance of the changes in the flow pattern around the upstream and downstream halves of the cylinder. With further increase of rotative speed, it is seen (Fig. 17) that the streamlines from the high velocity side wrap farther and farther around the cylinder. It seems probable that as the stagnation point moves back along the low velocity side, it will finally meet and merge with the point at which the two groups of streamlines reunite. A completely different type of flow will naturally result and the rapid increase of drag and reduction in the rate of increase of lift are its characteristics.

The fact that the power input is smaller with moving than stationary air indicates a reduction of air friction. This would be expected as the relative velocity of air to cylinder is reduced, around most of the circumference, by the rotation.

The characteristics of the cross cylinder, throughout the range covered, were very irregular. The relatively high power required to rotate this model prevented the reaching of high values of r .

However, in the upper portion of the speed range, the data were fairly consistent and as an L/D ratio of 5.5 was attained at $r = 1.8$, it would not be at all surprising if the maximum L/D ratio for this cylinder were found to be larger than that for the circular one.

The hysteresis effect found at low values of r has received no explanation, but it may be mentioned that the lower values (dashed curve in Fig. 7) were observed when the rotative speed was increasing, airspeed being held constant; as the rotative speed was reduced, the points on the upper curve were obtained.

While the curve of C_{OW} vs. r , for the cross cylinder, is rather erratic, if the portion between $r = 1.0$ and 1.8 were projected as far as the r axis, the intersection would occur at $r = 0.5$. The slope of this section of the curve is identical with that of the first portion of the corresponding curve for the circular cylinder.

The power consumption of the cross cylinder is greater in moving than in still air at values of r greater than 1.0 but less at smaller ratios.

The results from the tests of the compound strut cover a very limited range. The slopes of the curves of C_{OW} vs. r are much lower than the preceding ones, even though the coefficients were computed on the basis of projected area of the cylinder rather than the transverse projection of the strut.

As regards L/D ratio, the smaller gap is best and it is felt

that if it had been possible to use still smaller clearance and practically eliminate any flow through the gap, much better results might have been realized. It is evident that with any appreciable gap, the circulation around the entire assembly is reduced by the flow between the cylinder and fairing.

It will be seen that lift appears at the smallest values of r observed.

Conclusions

The controlled combination of translational and circulatory velocities has shown that -

1. The air forces obtainable by superposition of a circulatory flow upon the one arising from translation of a doubly symmetric body are several times greater than have ever been observed on any unsymmetric body.

2. Lift increases with circulation, although the law connecting the variables is not definitely established or its limits of application known.

3. The rate of increase of lift with rate of revolution seems practically independent of the shape of the rotating body, provided it is symmetrical about both axes in its plane of rotation, except at the very low speeds.

4. The drag of a blunt body in rectilinear air flow may be considerably reduced by the addition of a circulatory flow. (It seems probable that this results in a reduction in the width of the

turbulent area behind the cylinder before any "downwash" or change in the direction of the discharged airstream appears. This is in accord with the Karman theory of resistance as given in Joukowski's "Aerodynamique," p.203).

Bibliography

Reference 1 - Technical Report No. 116: Applications of Modern Hydrodynamics to Aeronautics, by L. Prandtl. 1921.

Table I
Circular Cylinder

R.P.M.	$\frac{D}{kg}$	$\frac{C_W}{kg}$	C_D	C_{CW}	$\frac{V}{(m/s)}$	r
25	1.136	-.010	.925	-.008	15	.010
500	1.136	+.010	.925	-.008	15	.300
900	1.026	-.020	.835	-.016	15	.360
1020	.942	-.022	.766	-.018	15	.408
1115	.852	-.007	.693	-.006	15	.460
1240	.777	+.003	.632	+.002	15	.496
1300	.754	.018	.614	.014	15	.520
1300	.747	.043	.608	.035	15	.520
1400	.740	.150	.602	.122	15	.560
1500	.744	.283	.605	.230	15	.600
1500	.740	.305	.602	.248	15	.600
1600	.744	.400	.605	.326	15	.640
1600	.744	.453	.605	.369	15	.640
1700	.759	.608	.618	.495	15	.680
1700	.751	.625	.611	.508	15	.680
1700	.750	.598	.610	.487	15	.680
1780	.751	.660	.611	.537	15	.712
1800	.754	.673	.614	.548	15	.720
1900	.757	.798	.616	.650	15	.760
1900	.751	.815	.611	.663	15	.760
1900	.757	.759	.616	.617	15	.760
2000	.759	.873	.618	.710	15	.800
2080	.765	.868	.622	.706	15	.832
2100	.764	.997	.622	.811	15	.840
2200	.764	1.073	.622	.873	15	.880
2220	.787	1.158	.640	.942	15	.888
2300	.772	1.188	.628	.967	15	.920
2420	.754	1.278	.614	1.040	15	.968
2500	.742	1.338	.604	1.089	15	1.000
2600	.729	1.468	.593	1.194	15	1.040
2620	.724	1.303	.589	1.060	15	1.048
2700	.710	1.578	.578	1.284	15	1.080
1300	.353	+.308	.646	.563	10	.780
1500	.351	.418	.642	.764	10	.900
1700	.338	.636	.618	1.163	10	1.020
1900	.331	.758	.605	1.386	10	1.140
2100	.322	.978	.589	1.789	10	1.260
2300	.324	1.083	.593	1.930	10	1.380
2500	.332	1.293	.607	2.362	10	1.500
2700	.334	1.403	.611	2.564	10	1.620
2900	.346	1.443	.633	2.639	10	1.740

Table I - Continued.

Circular Cylinder

R.P.M.	$\frac{D}{kg}$	$\frac{CWF}{kg}$	C_D	C_{CW}	$\frac{V}{(m/s)}$	r
1800	.085	.605	.622	4.43	5	2.16
2100	.105	.820	.769	6.00	5	2.51
2400	.130	.995	.952	7.28	5	2.87
2700	.151	1.110	1.105	8.13	5	3.23
3000	.168	1.170	1.230	8.57	5	3.59
3300	.188	1.250	1.376	9.15	5	3.95
3600	.196	1.295	1.434	9.48	5	4.32
1800	.167	.660	.624	2.46	7	1.54
2100	.173	.860	.646	3.21	7	1.79
2400	.181	1.140	.676	4.26	7	2.05
2700	.197	1.365	.736	5.10	7	2.30
3000	.222	1.700	.829	6.35	7	2.56
3300	.256	1.945	.956	7.26	7	2.82
3600	.287	2.210	1.070	8.25	7	3.07

$$S = 0.1741 \text{ m}^2$$

$$q = 1.535 \text{ kg/m}^2 (5 \text{ m/s}), 3.01 \text{ kg/m}^2 (7 \text{ m/s}), 6.15 \text{ kg/m}^2 (10 \text{ m/s})$$

and $13.81 \text{ kg/m}^2 (15 \text{ m/s})$.

Table II

Power Consumption of Circular Cylinder

Airspeed = 0

Airspeed = m/s

R.P.M.	Watts	R.P.M.	Watts
290	6.0	1020	14.5
580	10.0	1115	15.5
885	11.5	1240	17.3
1190	19.0		
1400	24.0	1500	23.8
1775	27.0	1700	26.0
2260	40.1	1900	28.4
2810	51.8	2080	31.8
3140	68.0	2220	28.6
3475	89.2	2300	30.2
		2420	31.9
		2500	33.6
		2600	34.8
		2700	37.2
		3000	44.8

Table III
Cross Cylinder

R.P.M.	$\frac{D}{\text{kg}}$	$\frac{CWF}{\text{kg}}$	C_D	C_{CW}	$\frac{V}{(\text{m/s})}$	r
0	.594	+.018	1.087	.033	10	.000
150	.723	.175	1.322	.320	10	.090
150	.740	.175	1.353	.320	10	.090
200	.763	.163	1.396	.298	10	.120
200	.782	.165	1.430	.302	10	.120
300	.702	.355	1.284	.649	10	.180
300	.731	.305	1.337	.557	10	.180
400	.618	.430	1.130	.786	10	.240
400	.640	.465	1.170	.850	10	.240
500	.655	.530	1.198	.969	10	.300
600	.518	.475	.947	.868	10	.360
600	.585	.480	1.070	.878	10	.360
700	.564	.495	1.032	.905	10	.419
840	.548	.395	1.000	.722	10	.503
850	.562	.475	1.028	.868	10	.509
1000	.493	.205	.902	.375	10	.598
1000	.548	.485	1.000	.887	10	.598
1200	.458	.260	.837	.475	10	.718
1200	.515	.545	.941	.996	10	.718
1400	.420	.365	.768	.667	10	.838
1400	.472	.700	.862	1.280	10	.838
1600	.405	.435	.740	.796	10	.958
1600	.460	.795	.841	1.454	10	.958
1600	.465	.740	.850	1.353	10	.958
1800	.440	.850	.804	1.554	10	1.08
1800	.450	.940	.823	1.720	10	1.08
2000	.417	1.010	.762	1.847	10	1.20
2000	.428	1.095	.782	2.000	10	1.20
2200	.373	1.305	.682	2.420	10	1.32
2200	.402	1.220	.735	2.230	10	1.32
2400	.343	1.475	.627	2.695	10	1.44
2400	.374	1.425	.684	2.605	10	1.44
2600	.372	1.630	.680	2.980	10	1.56
2800	.372	1.860	.680	3.400	10	1.68
3000	.377	2.075	.689	3.790	10	1.80
1800	1.079	1.205	.879	.981	15	.720
2000	1.029	1.310	.838	1.067	15	.800
2200	.994	1.440	.810	1.174	15	.880
2400	.980	1.605	.798	1.307	15	.960
2600	.966	1.805	.787	1.470	15	1.040

$$S = 0.1741 \text{ m}^2$$

$$q = 6.15 \text{ kg/m}^2 (10 \text{ m/s}), \quad 13.81 \text{ kg/m}^2 (15 \text{ m/s})$$

Table IV

Power Consumption of Cross Cylinder

Airspeed = 0

Airspeed = 10 m/s

Airspeed = 15 m/s

R.P.M.	Watts	R.P.M.	Watts	R.P.M.	Watts
1000	16.1	140	6.3	1800	62.4
1200	23.8	300	10.4	2000	74.0
1400	35.0	600	18.0	2100	84.0
1600	42.0	1000	28.0	2200	88.3
1800	53.9	1300	35.0	2400	105.0
2000	66.6	1600	43.0	2600	131.0
2200	81.2	1800	48.0	2700	138.0
2400	96.6	2000	59.4		
2600	123.2	2200	72.0		
2800	153.2	2400	87.1		
		2600	112.5		
		2800	141.0		

Table V

Compound Strut
Gap = 1/8"

R.P.M.	$\frac{D}{\text{kg}}$	$\frac{CWF}{\text{kg}}$	C_D	C_{CW}	$\frac{V}{(\text{m/s})}$	r
0	.109	.000	.199	.000	10	0
55	.113	.003	.206	.005	10	.02
105	.114	.016	.208	.029	10	.06
150	.114	.020	.208	.036	10	.09
200	.115	.036	.210	.066	10	.12
250	.115	.068	.210	.124	10	.15
300	.115	.093	.210	.170	10	.18
350	.115	.133	.210	.243	10	.21
400	.117	.138	.214	.252	10	.24
450	.119	.193	.217	.352	10	.27
450	.119	.250	.217	.457	10	.27
500	.121	.218	.221	.398	10	.30
600	.125	.335	.228	.611	10	.36
800	.128	.278	.234	.508	10	.36
700	.128	.333	.234	.608	10	.42
900	.125	.375	.238	.685	10	.54
1200	.123	.440	.225	.803	10	.72
1500	.144	.635	.263	1.160	10	.90
1600	.149	.720	.272	1.314	10	.96
1700	.165	.730	.301	1.332	10	1.02
1900	.175	.730	.320	1.332	10	1.14
2100	.214	.770	.391	1.406	10	1.27
2400	.251	.890	.458	1.625	10	1.45
2700	.256	.920	.467	1.680	10	1.63
3000	.250	.885	.457	1.616	10	1.81
0	.565		.254		20	
500	.557	-.140	.255	.063	20	.15
700	.557	-.125	.255	.056	20	.21
900	.543	-.030	.245	.013	20	.27
900	.552	+.065	.249	.029	20	.27
1100	.533	+.110	.240	.050	20	.33
1200	.535	+.185	.241	.083	20	.36
1300	.530	.290	.239	.131	20	.39
1400	.537	.350	.242	.158	20	.42
1600	.515	.675	.232	.304	20	.48
1600	.530	.615	.239	.277	20	.48
1800	.532	.950	.240	.428	20	.592
2000	.532	1.025	.240	.462	20	.603

 $S = 0.1741 \text{ m}^2$ $q = 6.15 \text{ kg/m}^2$ (10 m/s), 13.81 kg/m^2 (20 m/s).

Table VI

Power Consumption of Compound Strut.
Gap = $1/8$ "

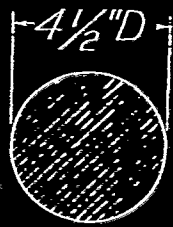
Airspeed = 0		Airspeed = 10 m/s	
R.P.M.	Watts	R.P.M.	Watts
100	2.1	100	2.8
300	3.0	300	4.0
500	5.6	500	5.6
800	7.6	800	9.5
1100	12.5	1100	15.6
1400	18.0	1400	18.6
1700	22.8	1700	25.9
2000	32.2	2000	35.2
2300	41.6	2300	40.8
2600	46.4	2600	45.6
2900	50.4	2900	53.6

Table VII
Compound Strut (3/8" Gap)

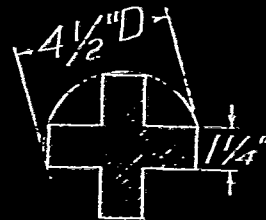
R.P.M.	$\frac{D}{\text{kg}}$	$\frac{CWF}{\text{kg}}$	C_D	C_{CW}	$\frac{V}{(\text{m/s})}$	r
500	.218	.288	.398	.526	10	.300
600	.211	.303	.386	.553	10	.360
700	.213	.318	.389	.581	10	.419
800	.218	.318	.398	.581	10	.480
900	.221	.363	.403	.663	10	.540
1200	.243	.563	.444	1.030	10	.718
1500	.288	.903	.526	1.650	10	.898
1800	.324	.913	.592	1.670	10	1.08
2100	.344	.938	.628	1.713	10	1.26
2400	.351	1.038	.641	1.900	10	1.44
2700	.351	1.078	.641	1.920	10	1.62
3000	.348	1.143	.635	2.090	10	1.80
3300	.339	1.143	.619	2.090	10	1.98

$$S = 0.1741 \text{ m}^2$$

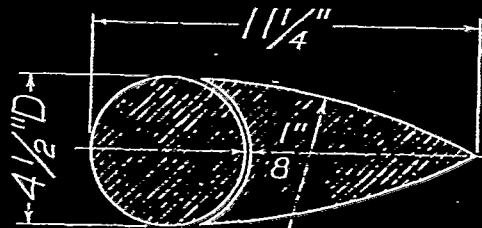
$$q = 6.15 \text{ kg/m}^2$$



Circular
cylinder



Cross
cylinder



Compound strut

19" R

Fig. 1 Section of cylinders and
struts used in tests.

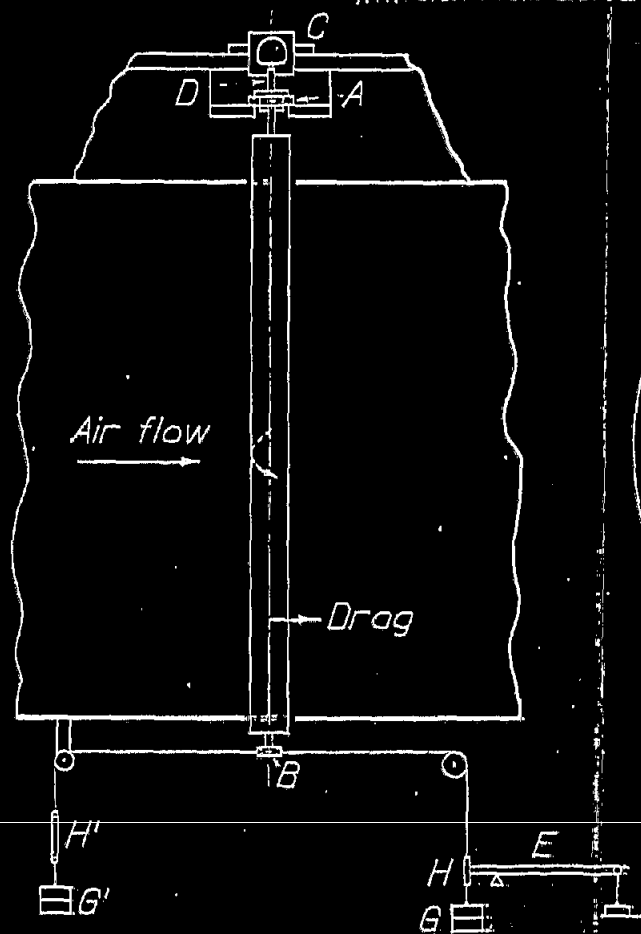


Fig. 2 Drag balance set up.

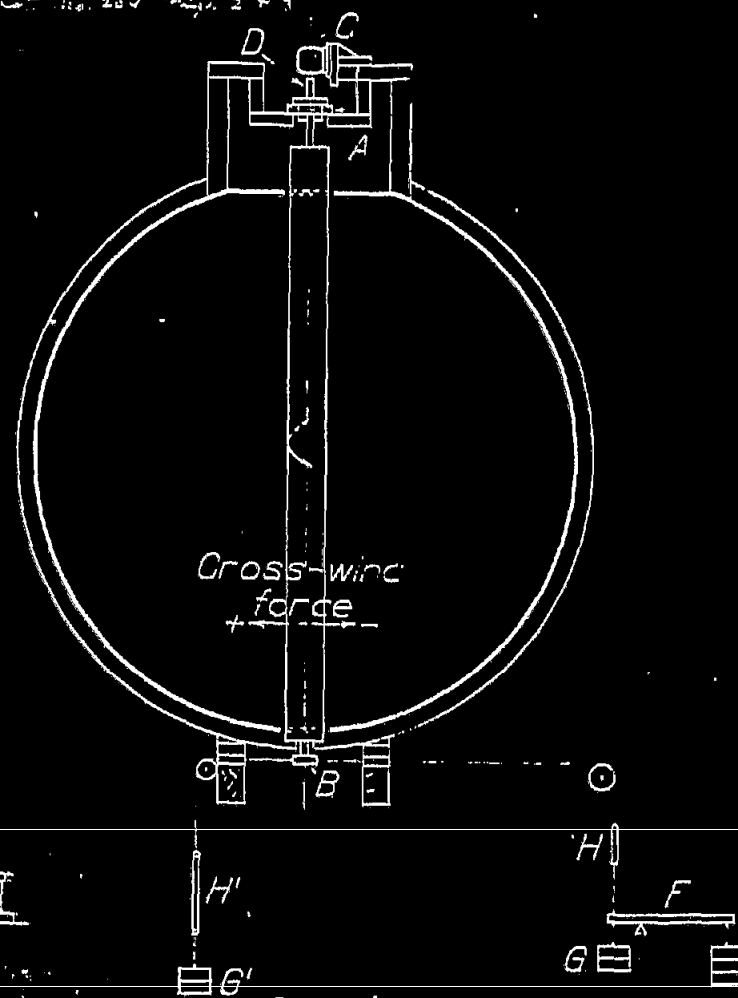


Fig. 3 Cross-wind force set up.

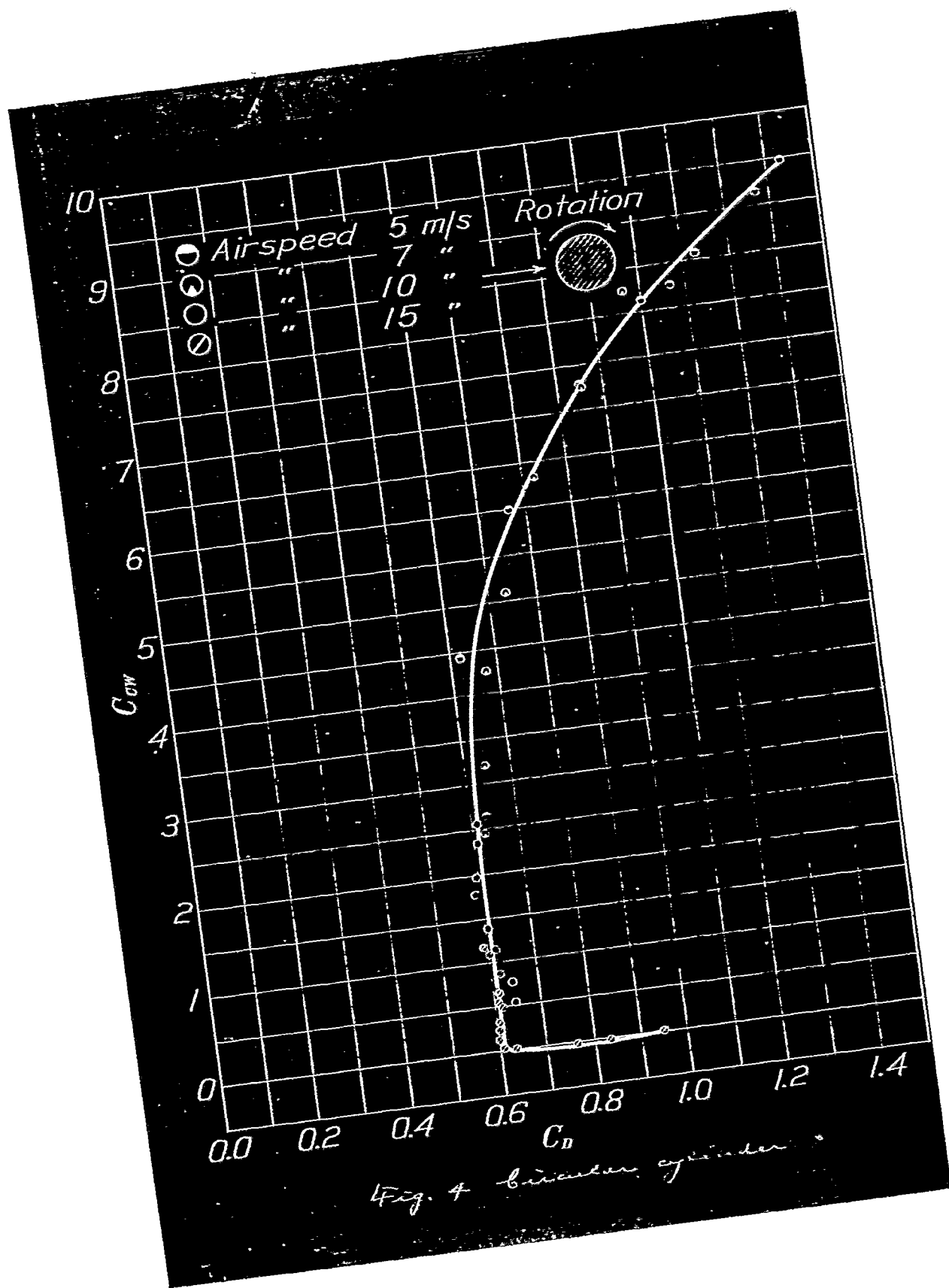


Fig. 4 circular cylinder

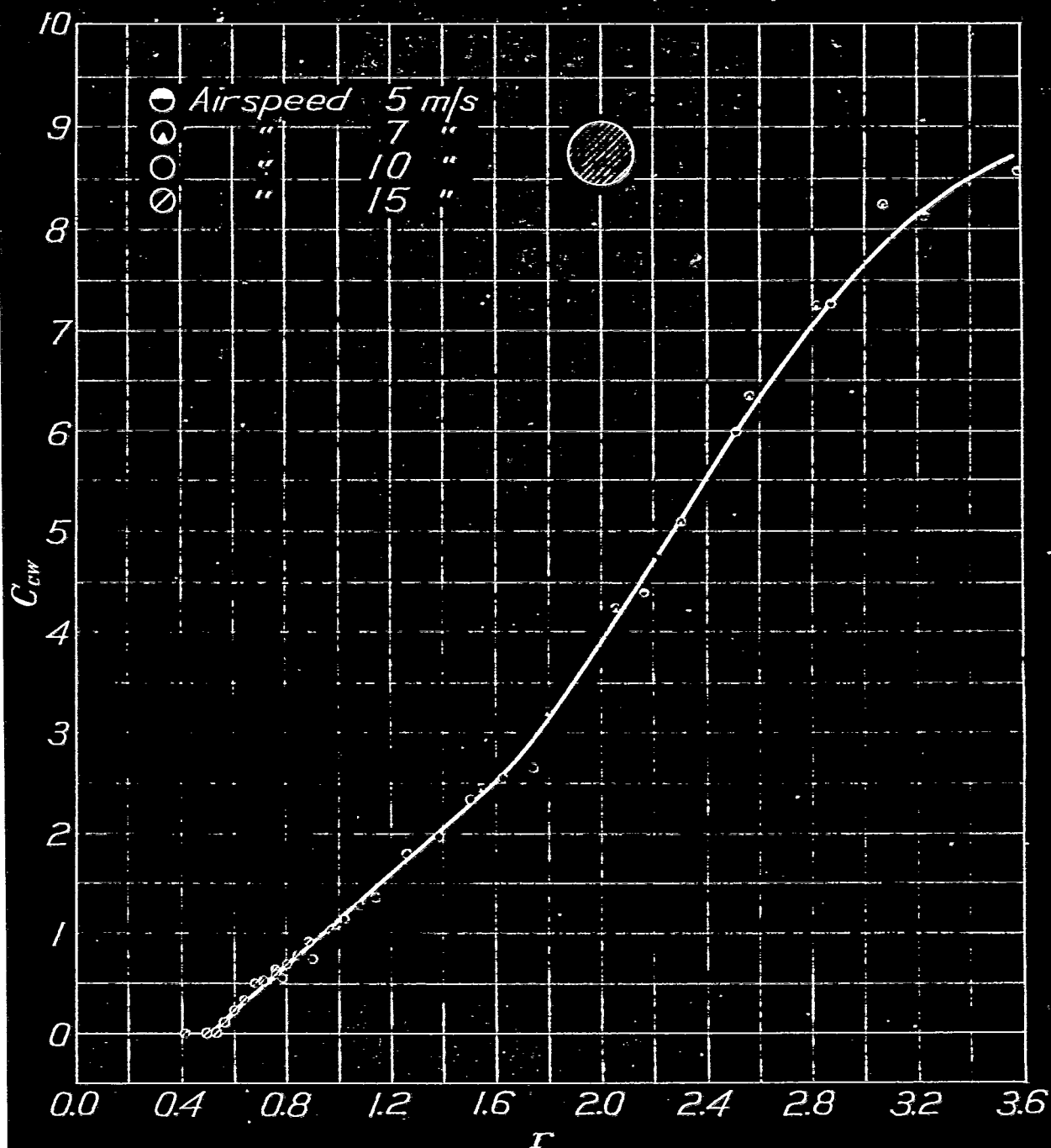


Fig. 5 Circular cylinder

N.A.C.A. Technical Note No. 204 Fig. 6

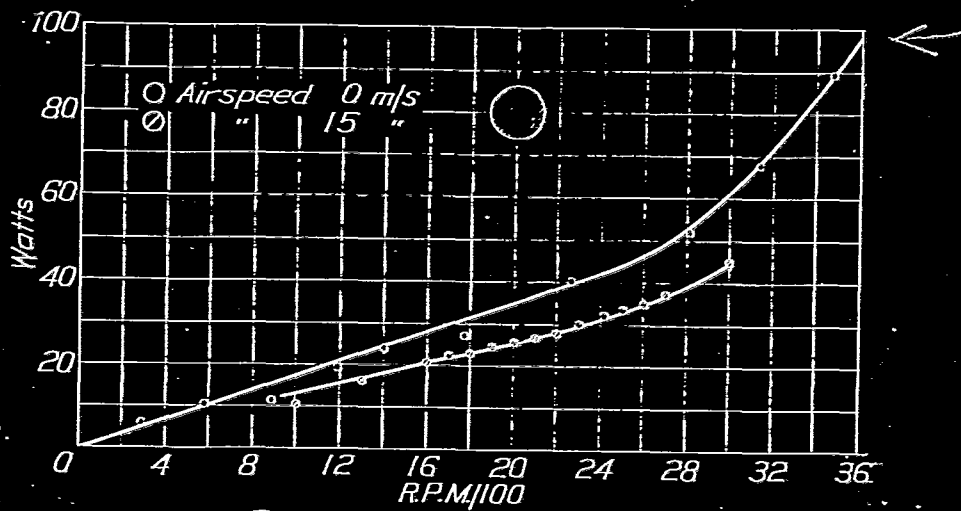


Fig. 6 Power consumption of circular cylinder.

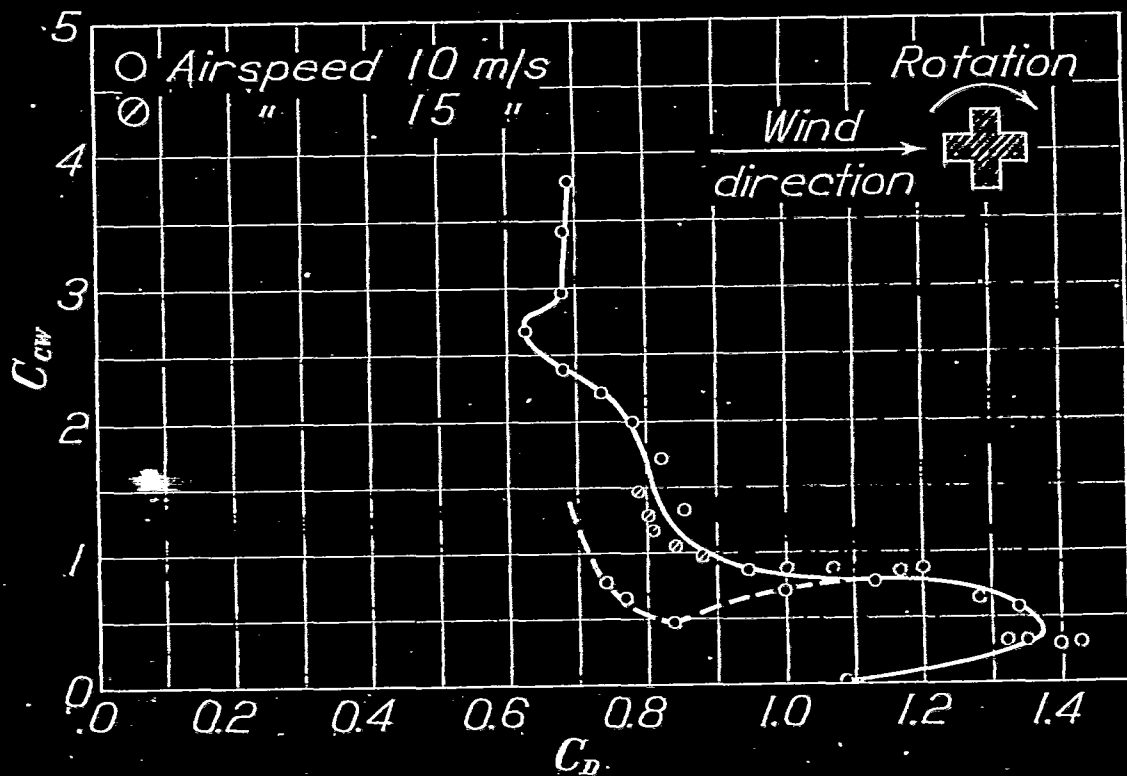


Fig. 7 Cross cylinder.

ical Note No 209 Fig. 7 & 8

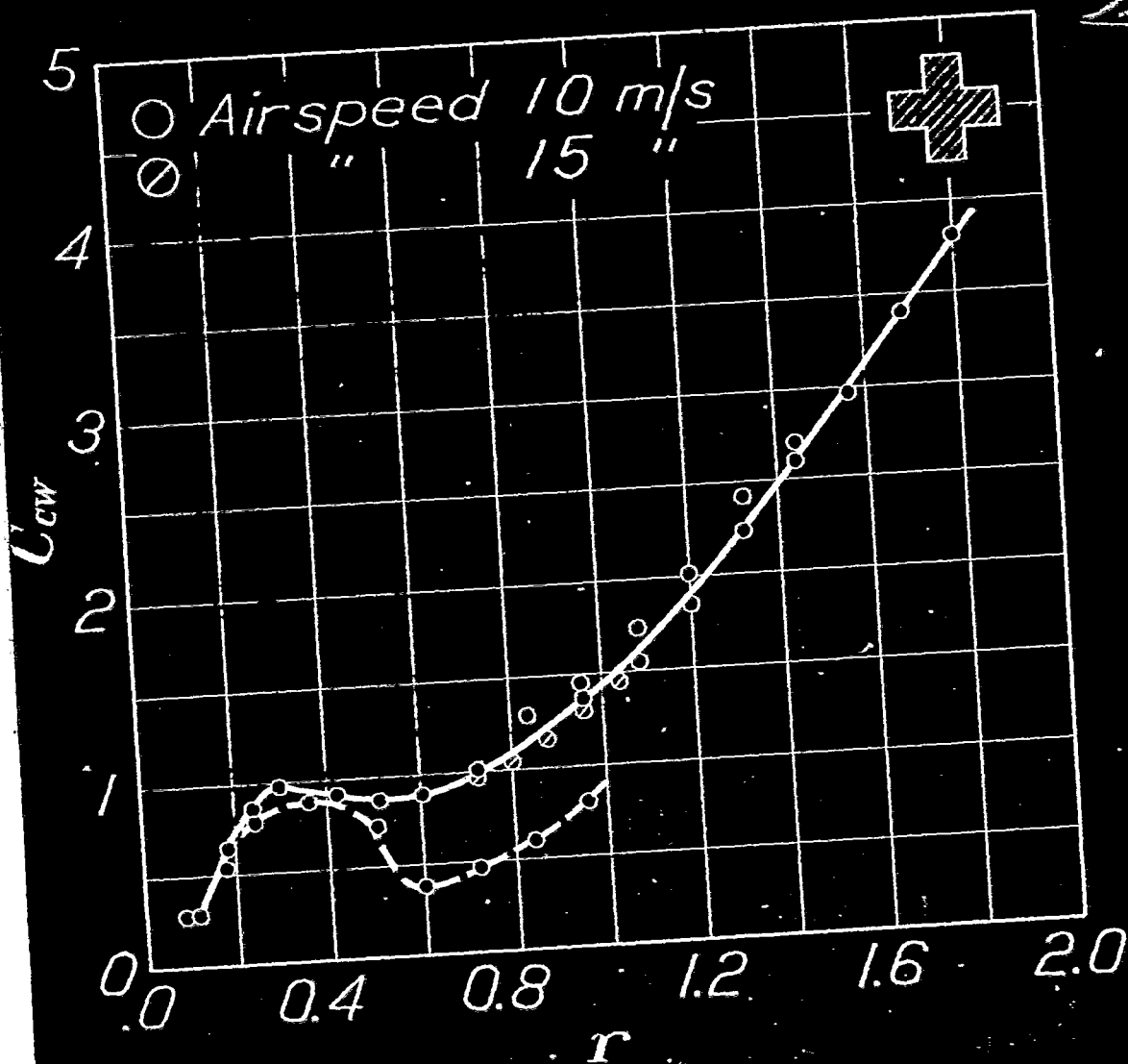


Fig. 8. Cross cylinder

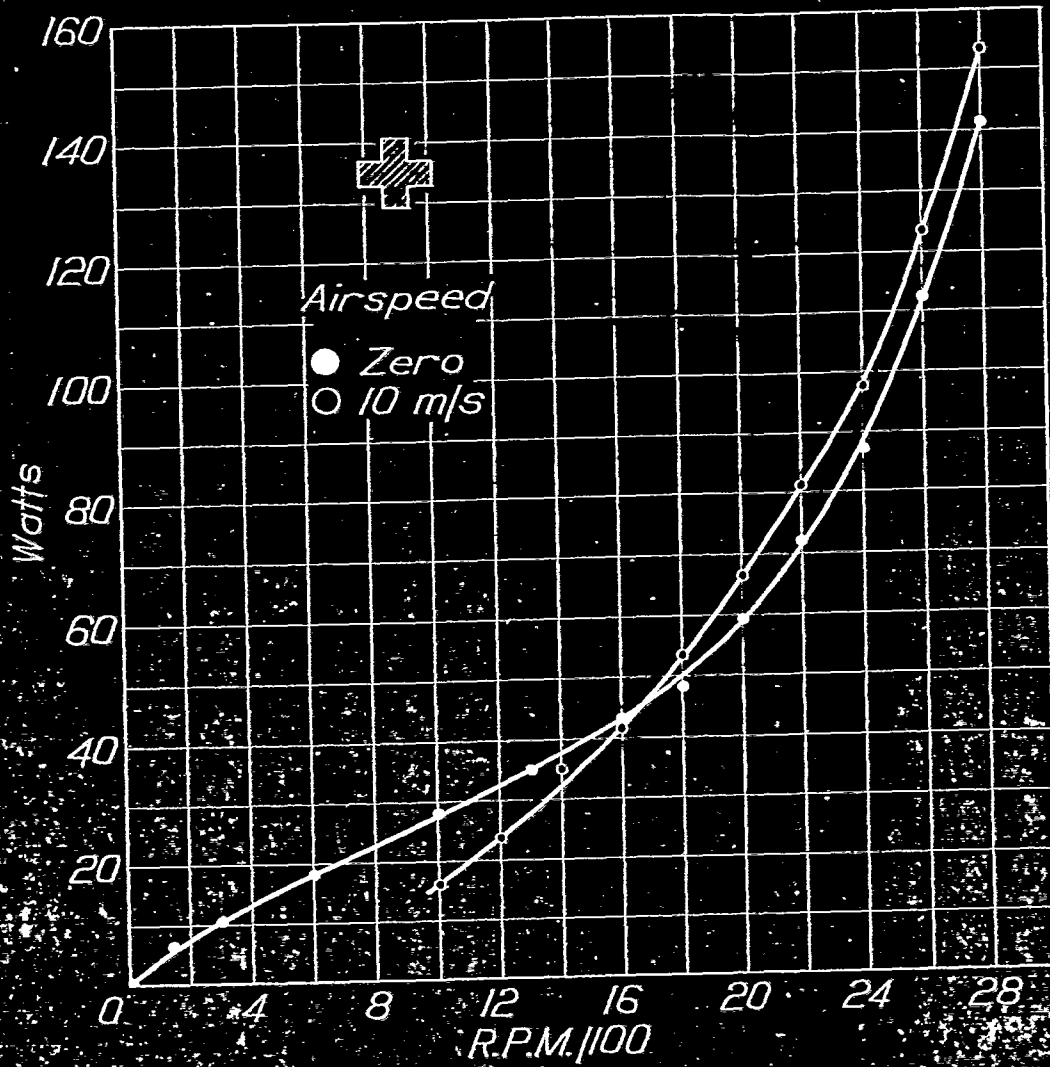


Fig. 9 Power consumption of case cylinder

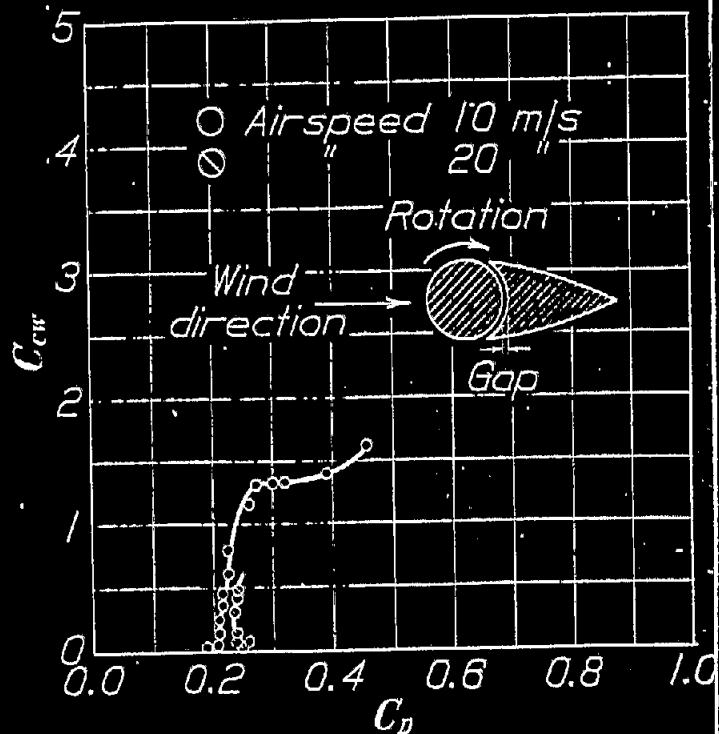


Fig. 10 Streamlined strut. Gap $\frac{1}{8}$ inch

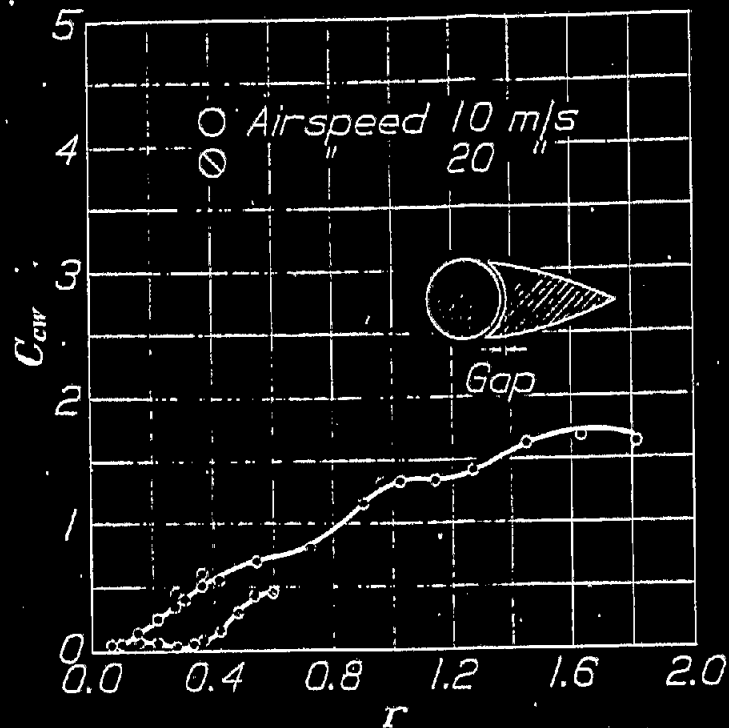


Fig. 11 Streamlined strut. Gap $\frac{1}{8}$ inch

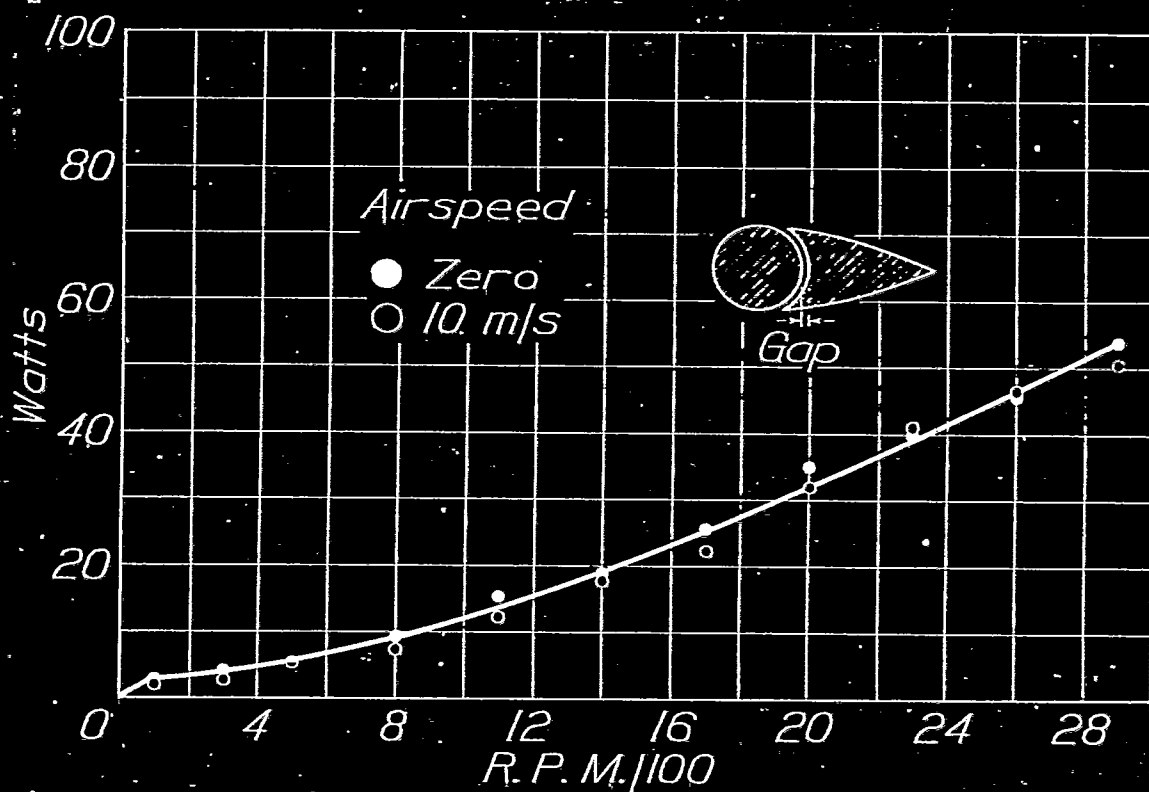


Fig. 12. Power consumption of combination strut.
Gap 1/8"

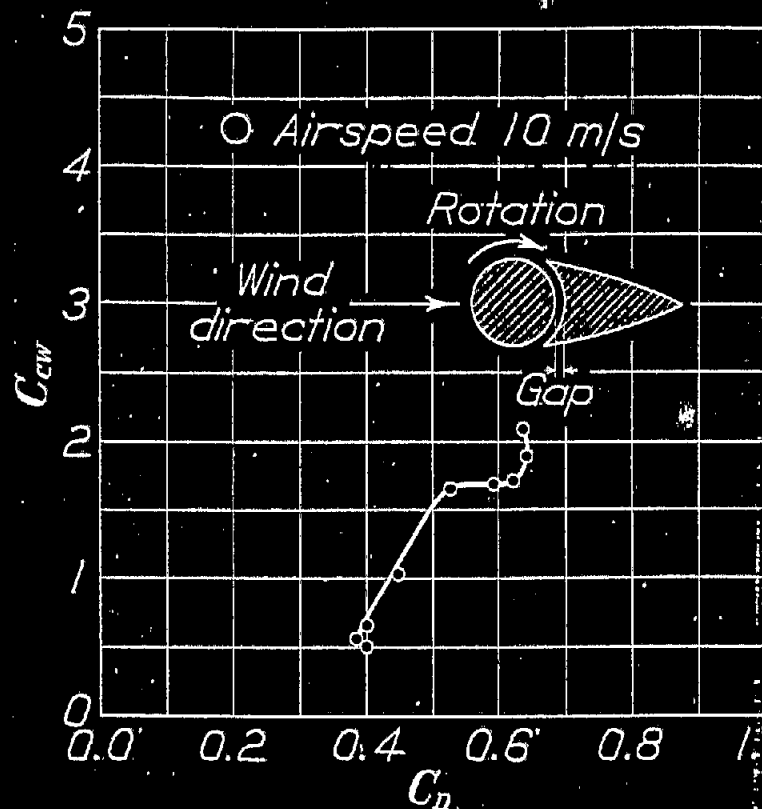


Fig. 13 Compounded strut, gap $\frac{3}{8}$ "

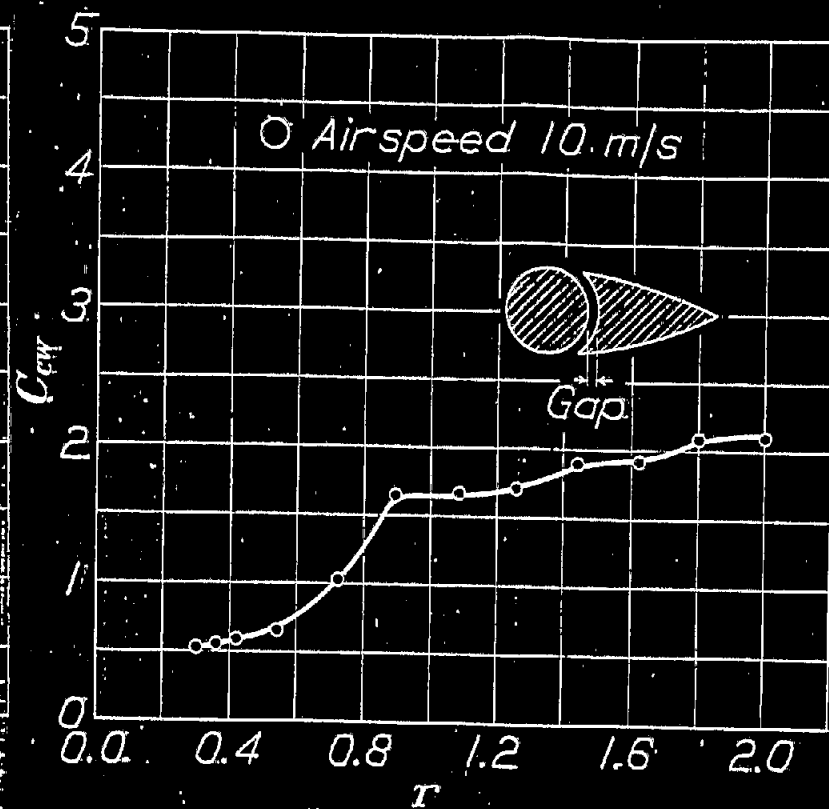


Fig. 14 Compounded strut, gap $\frac{7}{8}$ "

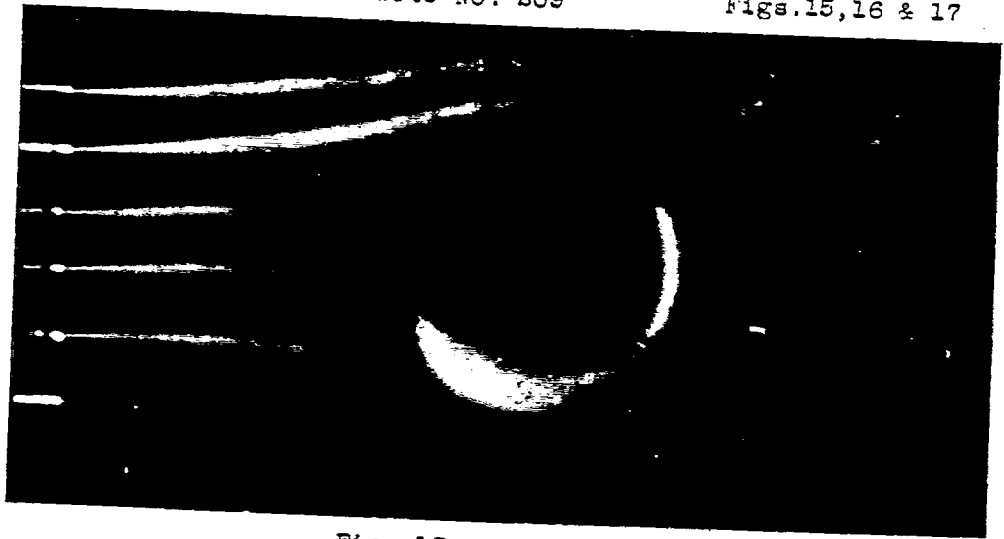


Fig. 15 600 R.P.M.



Fig. 16 1200 R.P.M.

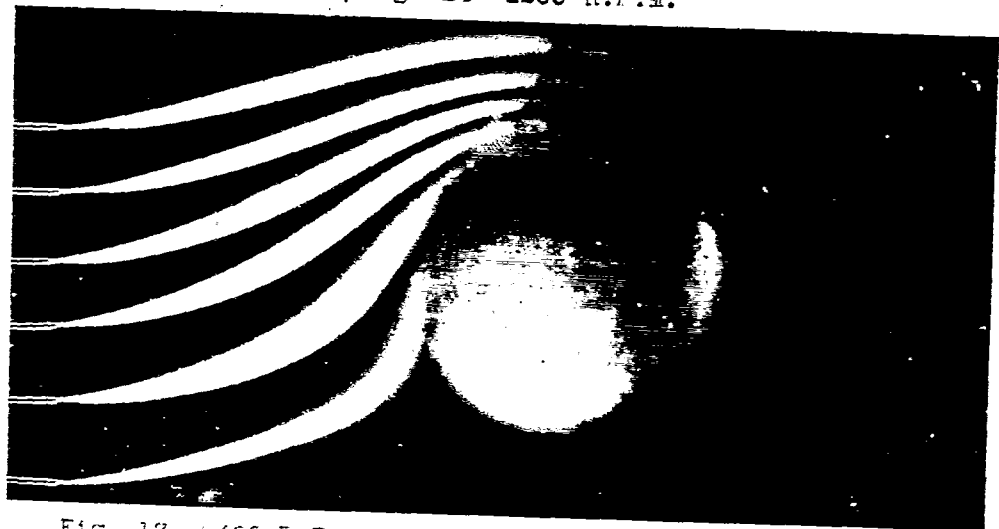
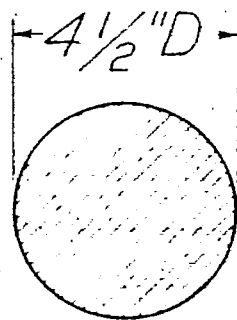


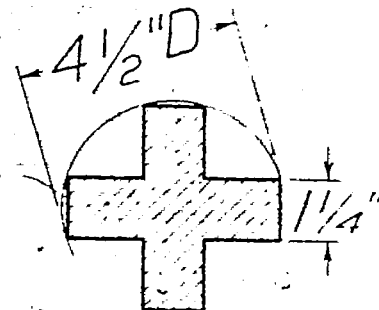
Fig. 17 2400 R.P.M.

Airspeed 5 m/s

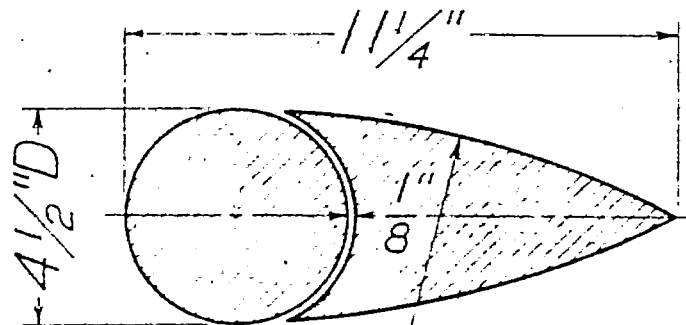
11884 A.S.



Circular
cylinder



Cross
cylinder



Compound strut

Fig. 1 Section of cylinders and
struts used in test.

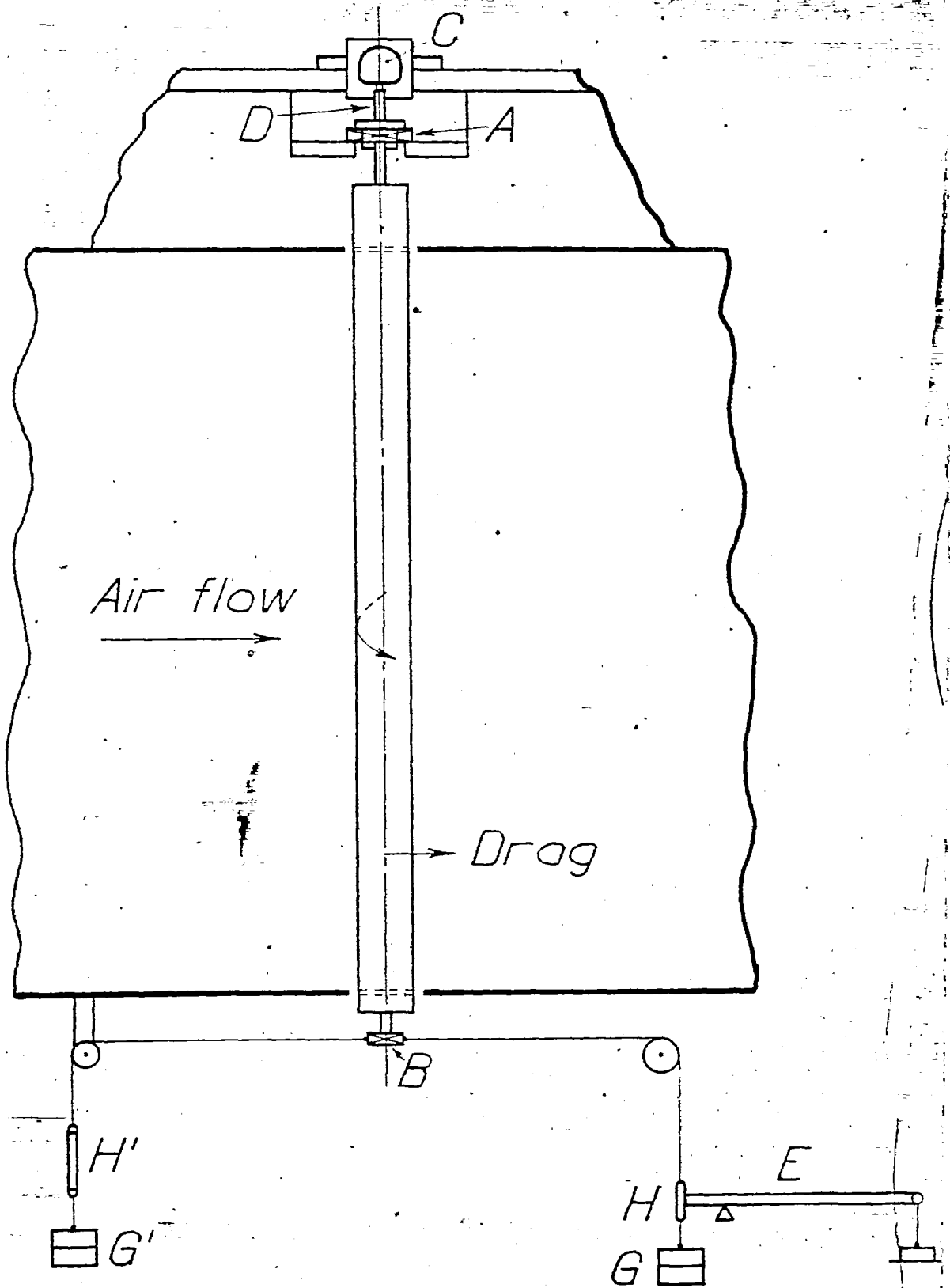


Fig. 2 Drag balance set up

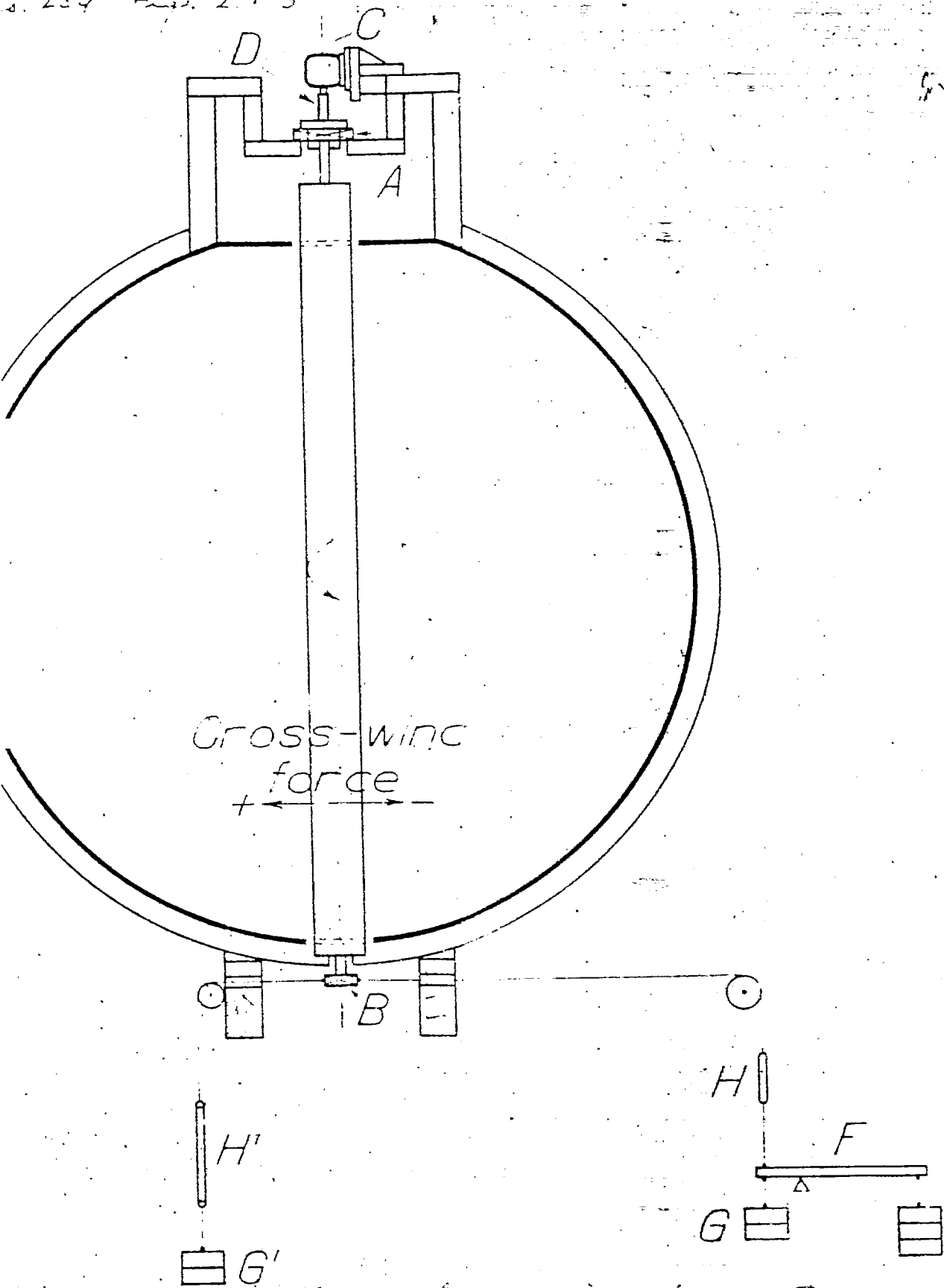


Fig. 3 cross-wind force set up.

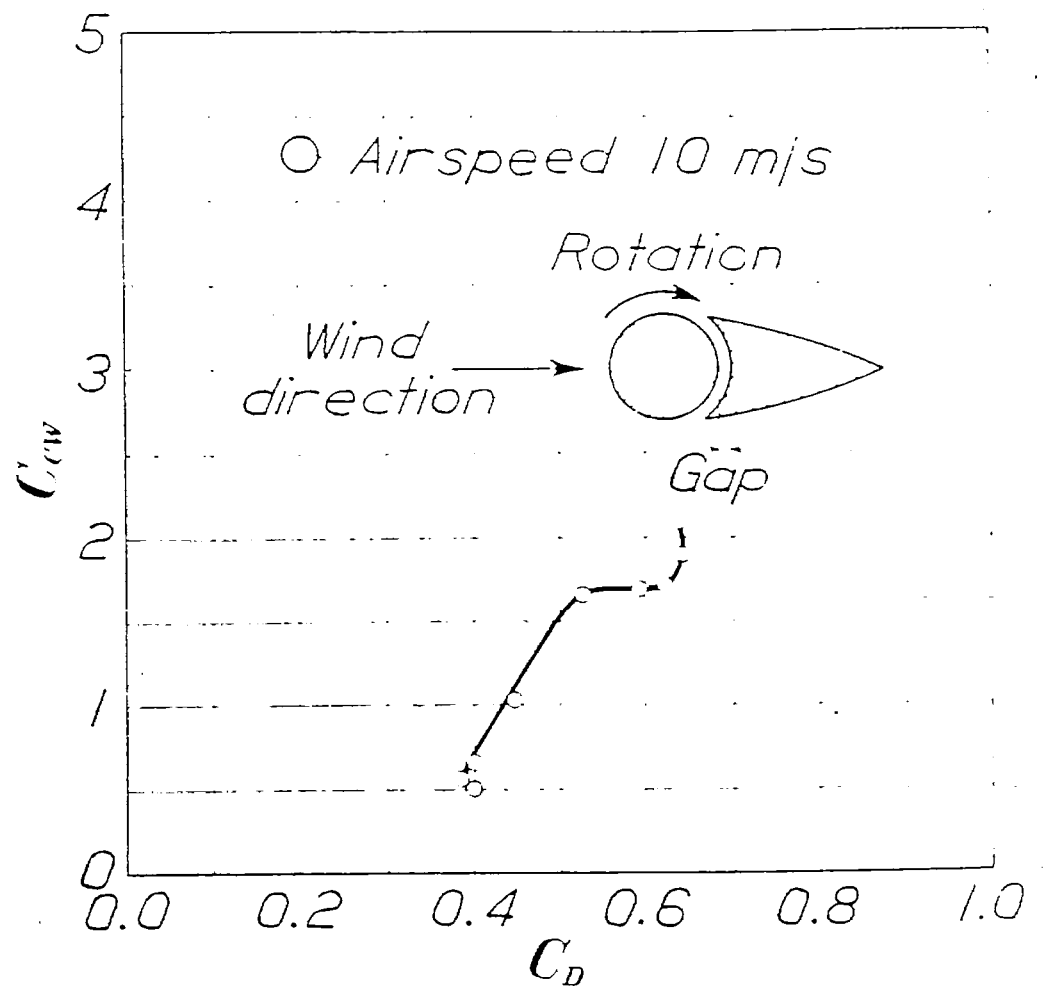
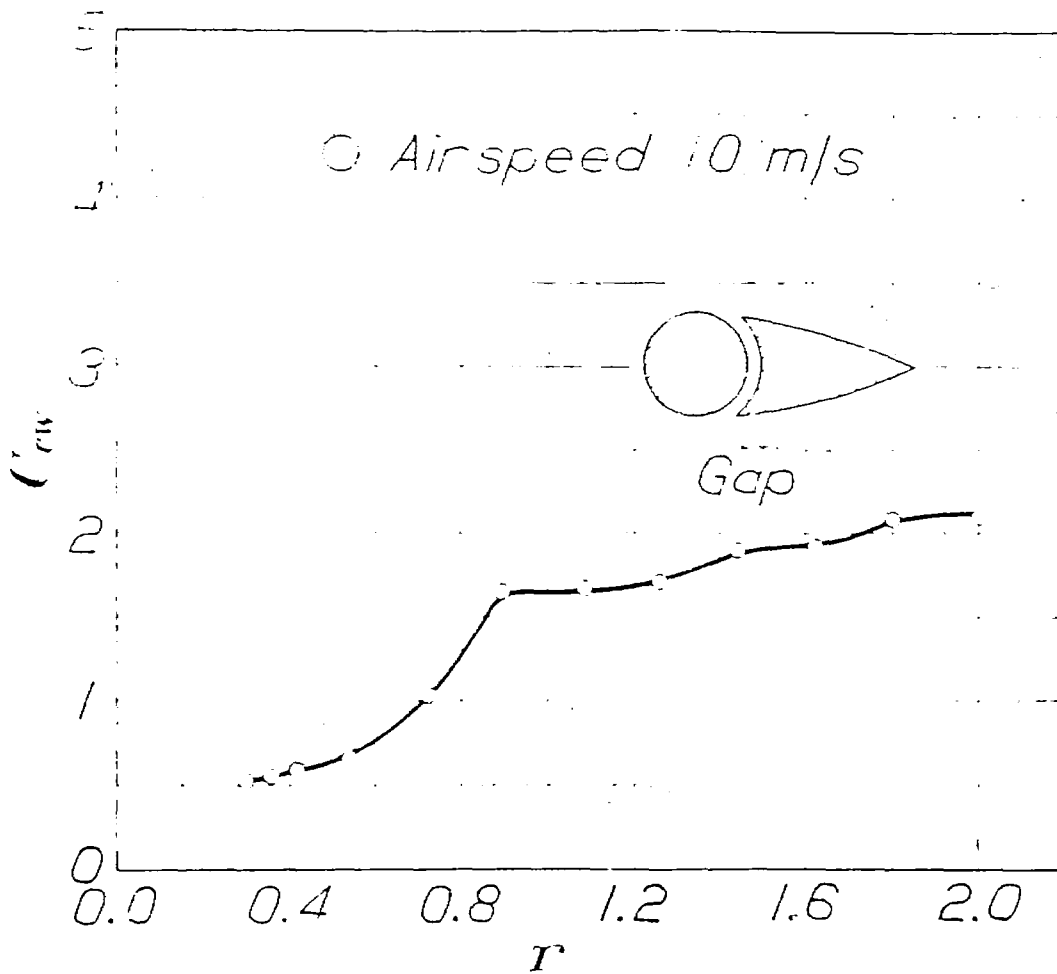
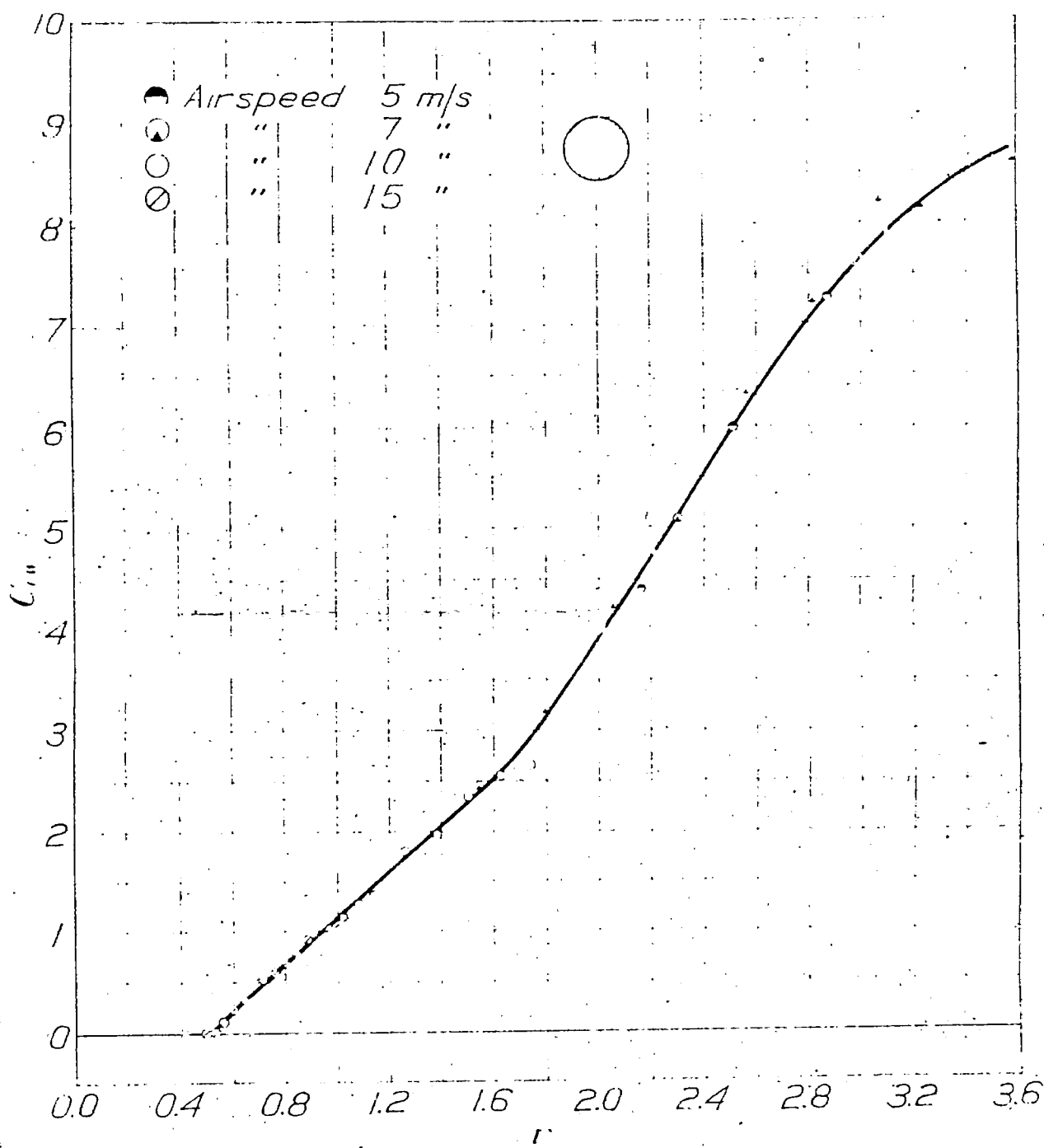


Fig. 3 compound start. $\dot{\theta} = 5$

Figure 1. Drag coefficient C_{Dw} vs. distance r for a sphere and a cone.



Gap = 0.001 m (0.039 in.)



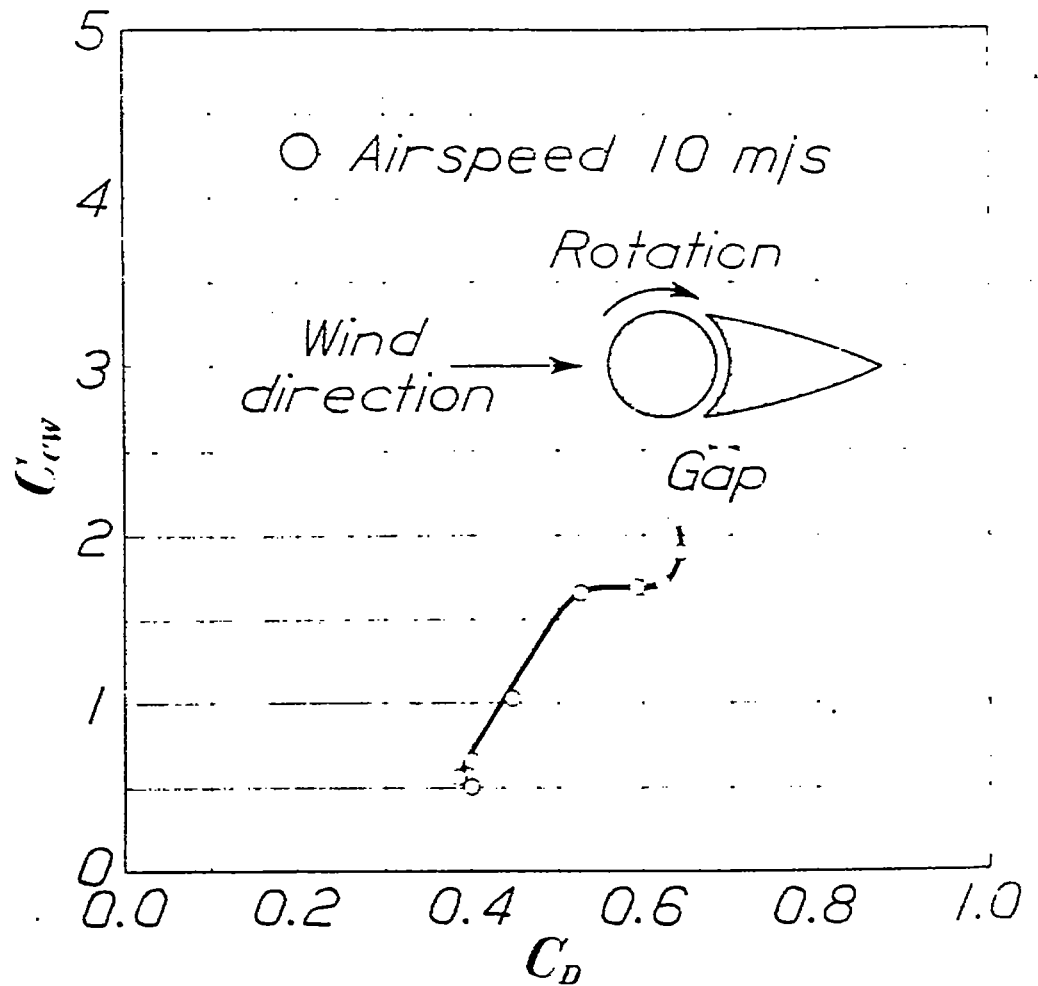
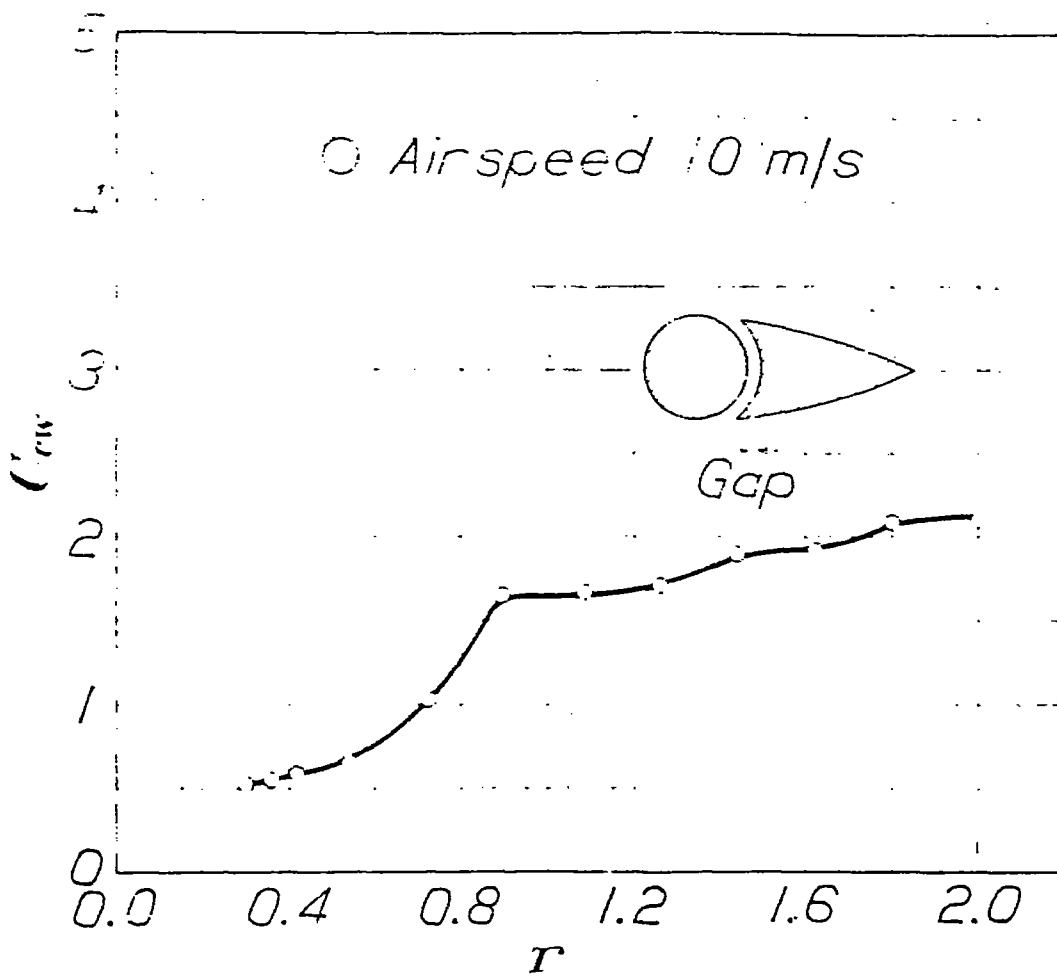
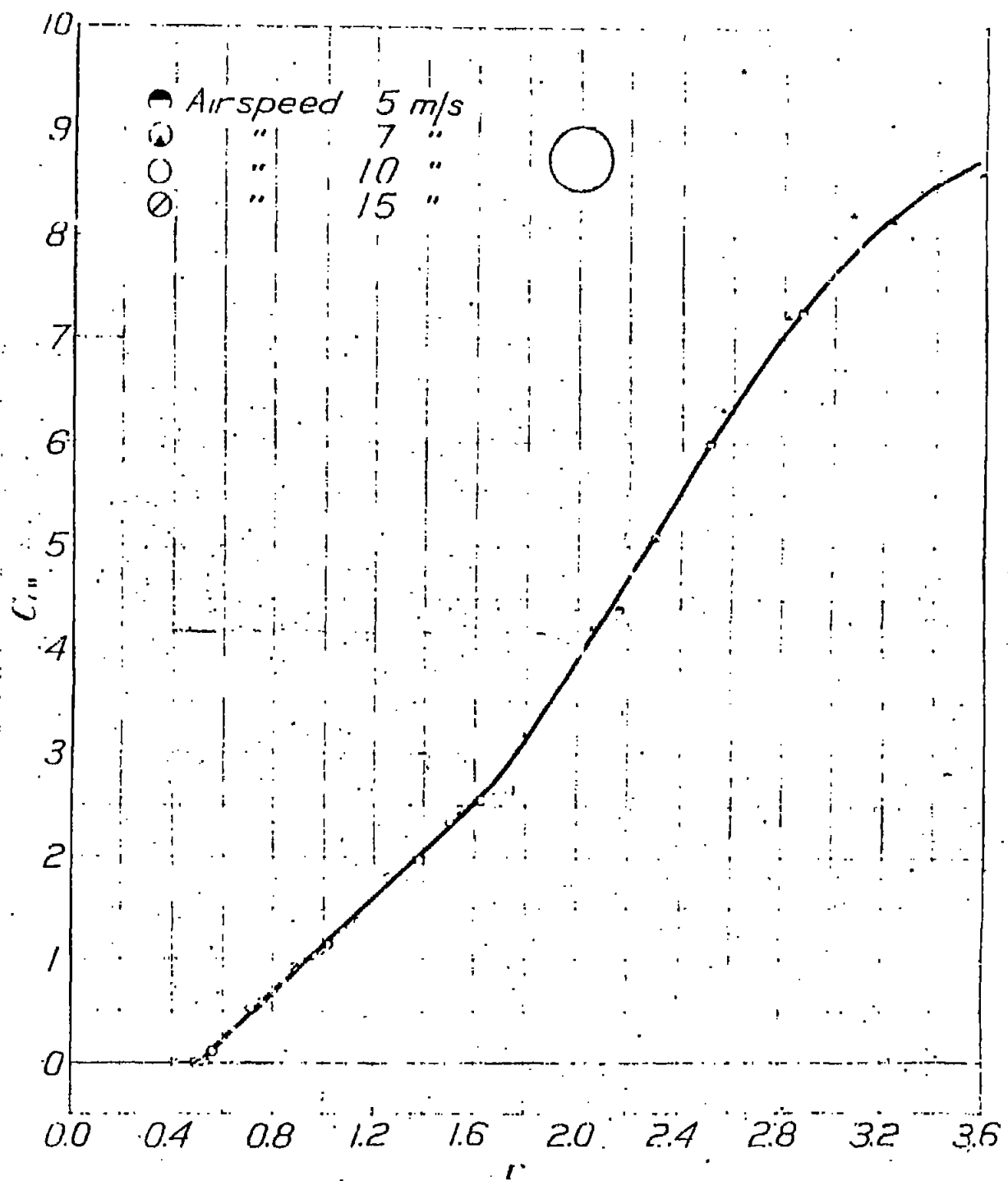


Fig. 3 Combined start, gap test

Wing planform: 100 mm span, 10 mm chord, 10 mm thickness



Wing planform: 100 mm span, 10 mm chord, 10 mm thickness



N.A.C.A. Technical Note No. 2041, Fig. 6

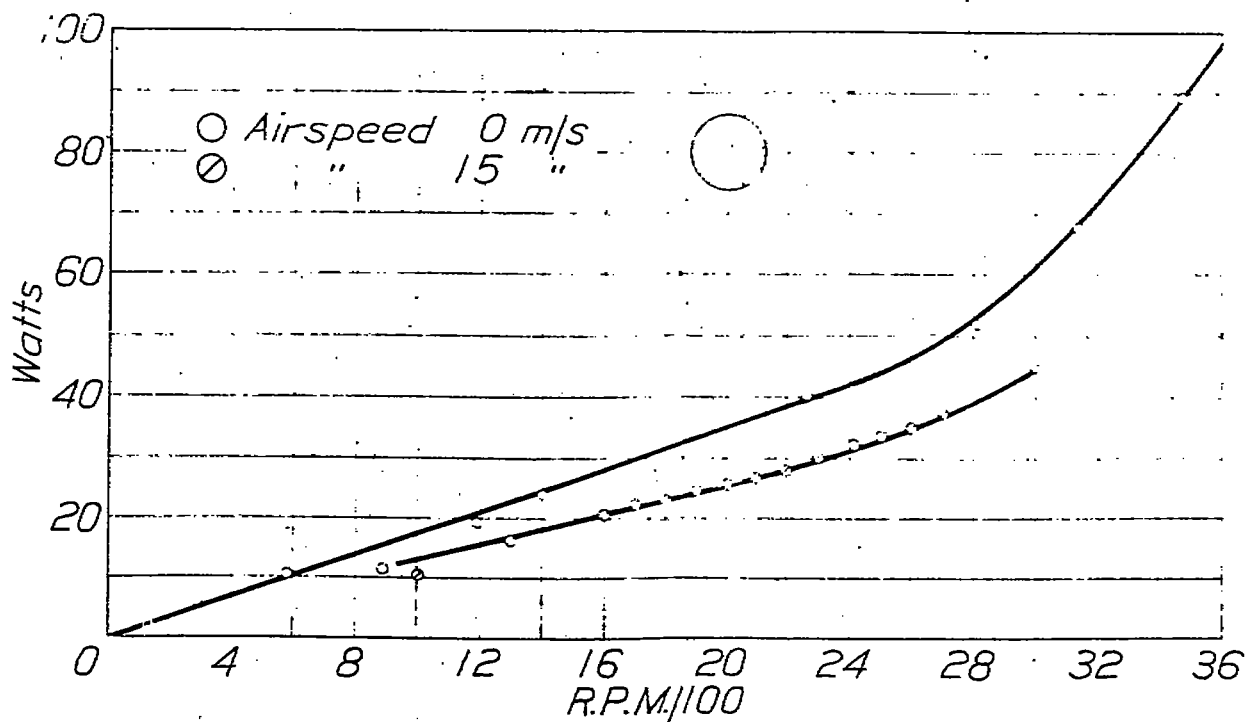
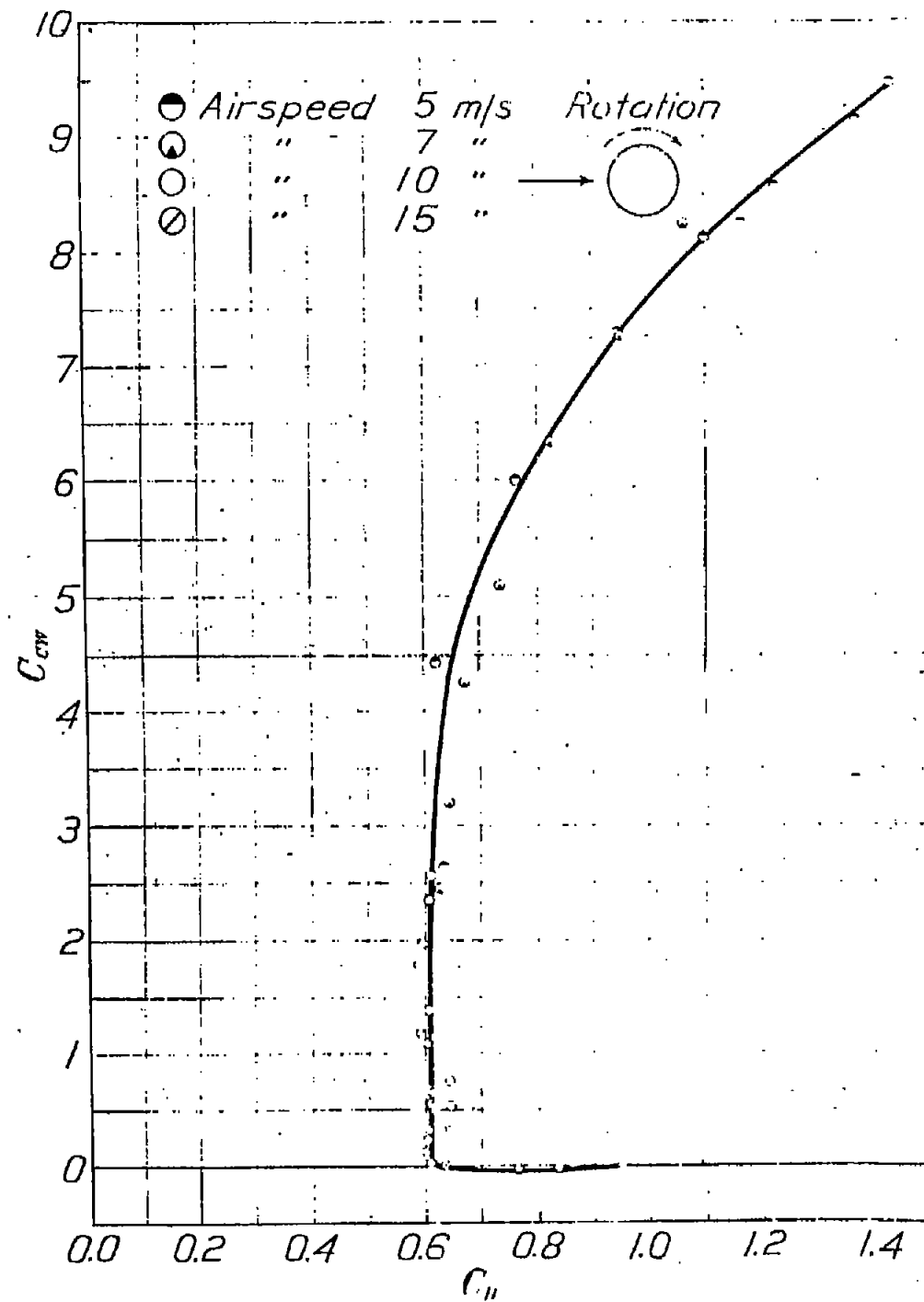


Fig. 6 Power consumption of aircraft propeller



Recal Mot. No. 204 Fig. 7 T. 8

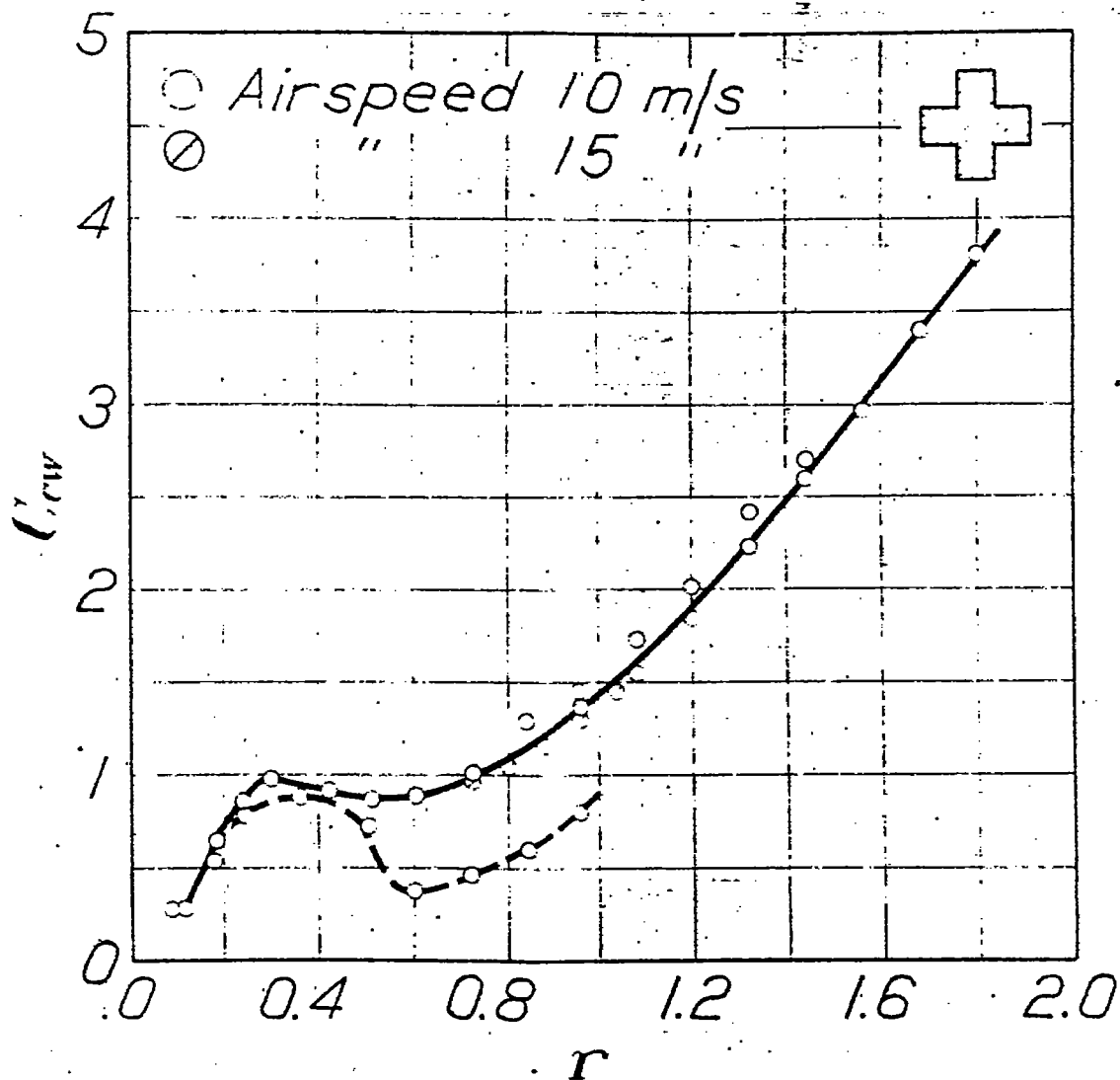


Fig. 8 Cross cylinders

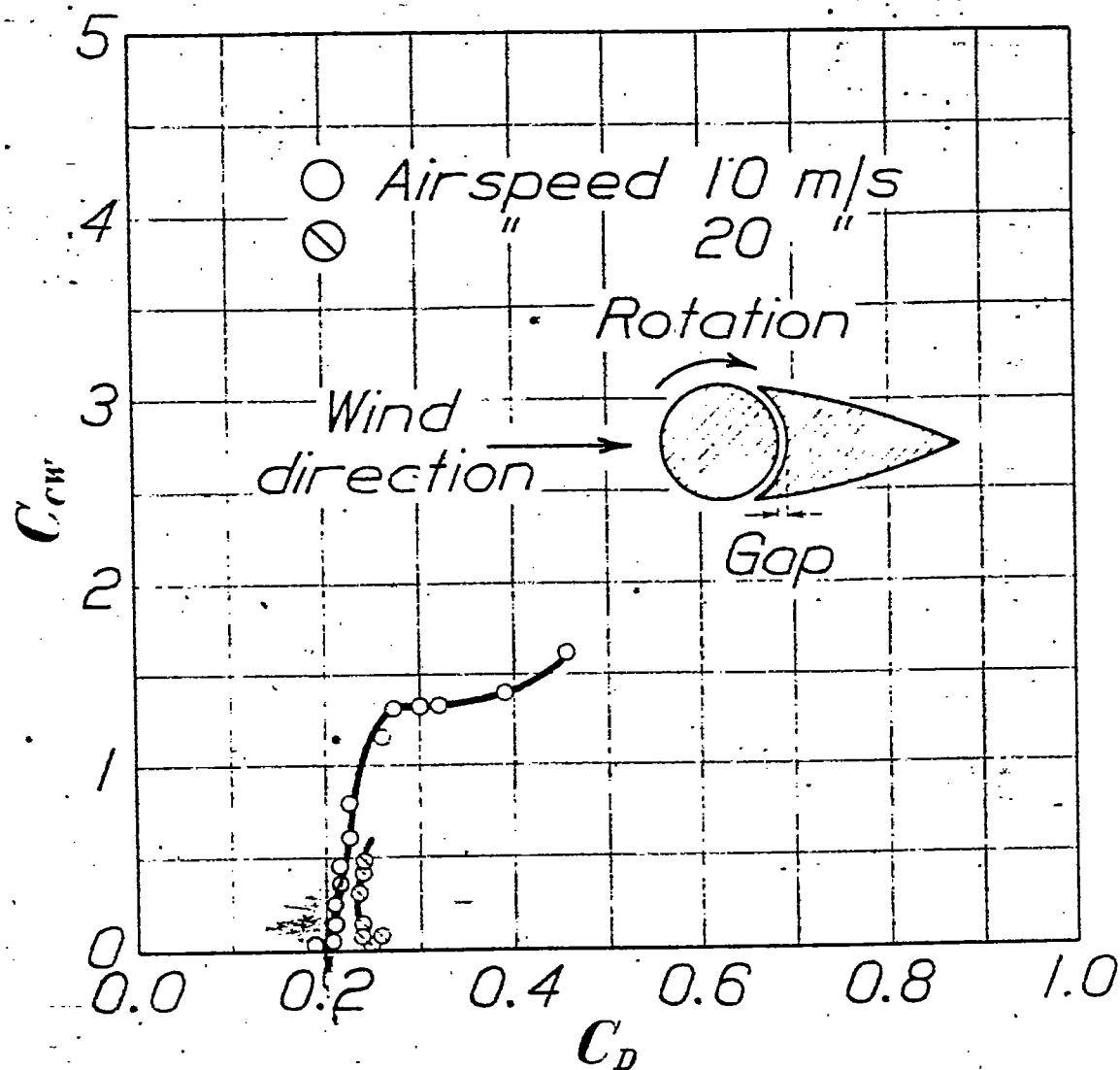


Fig. 10 Curved street. Gap 1/8"

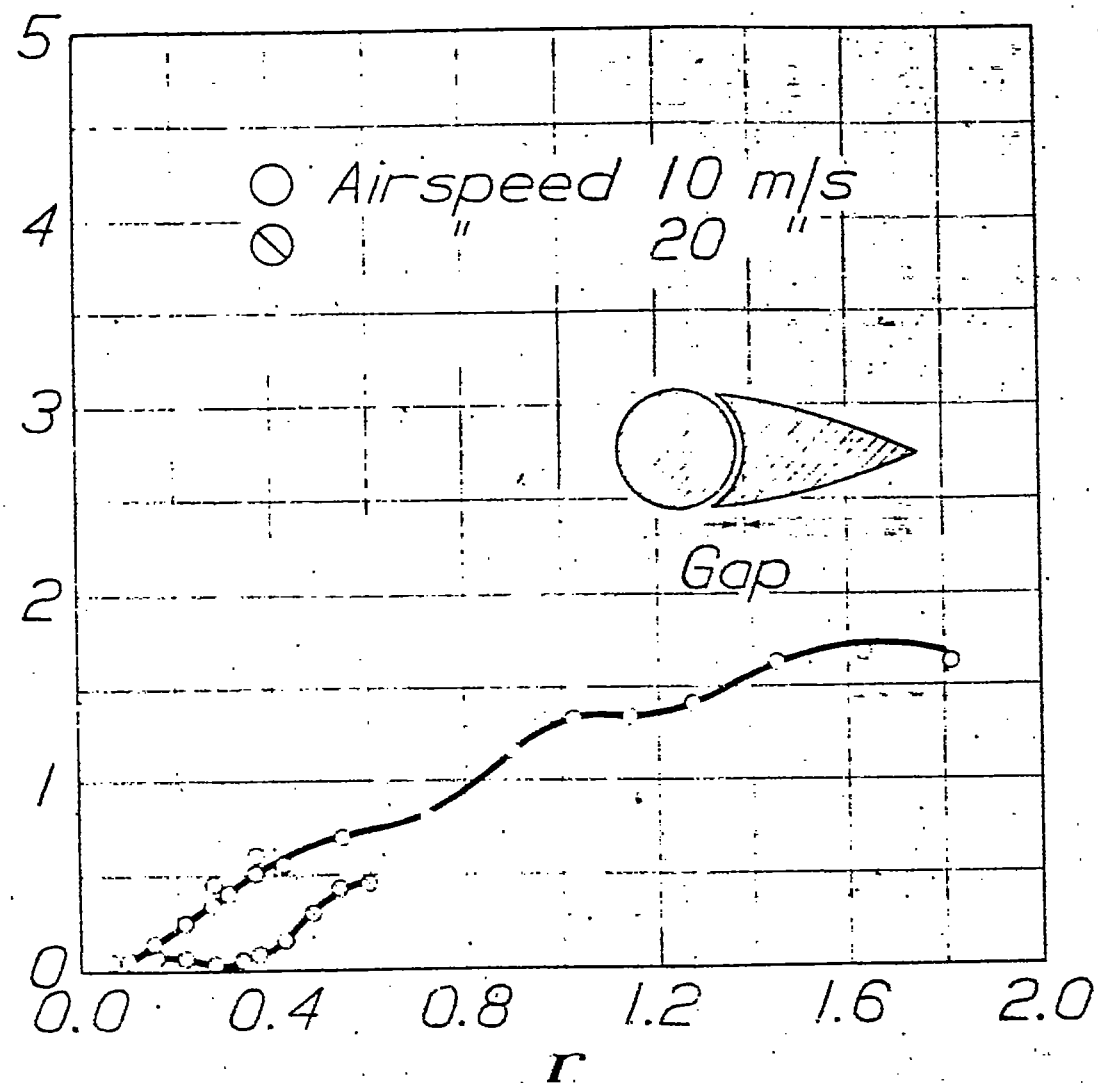


Fig. 11 Compound stut. Gap $\frac{1}{8}$ "

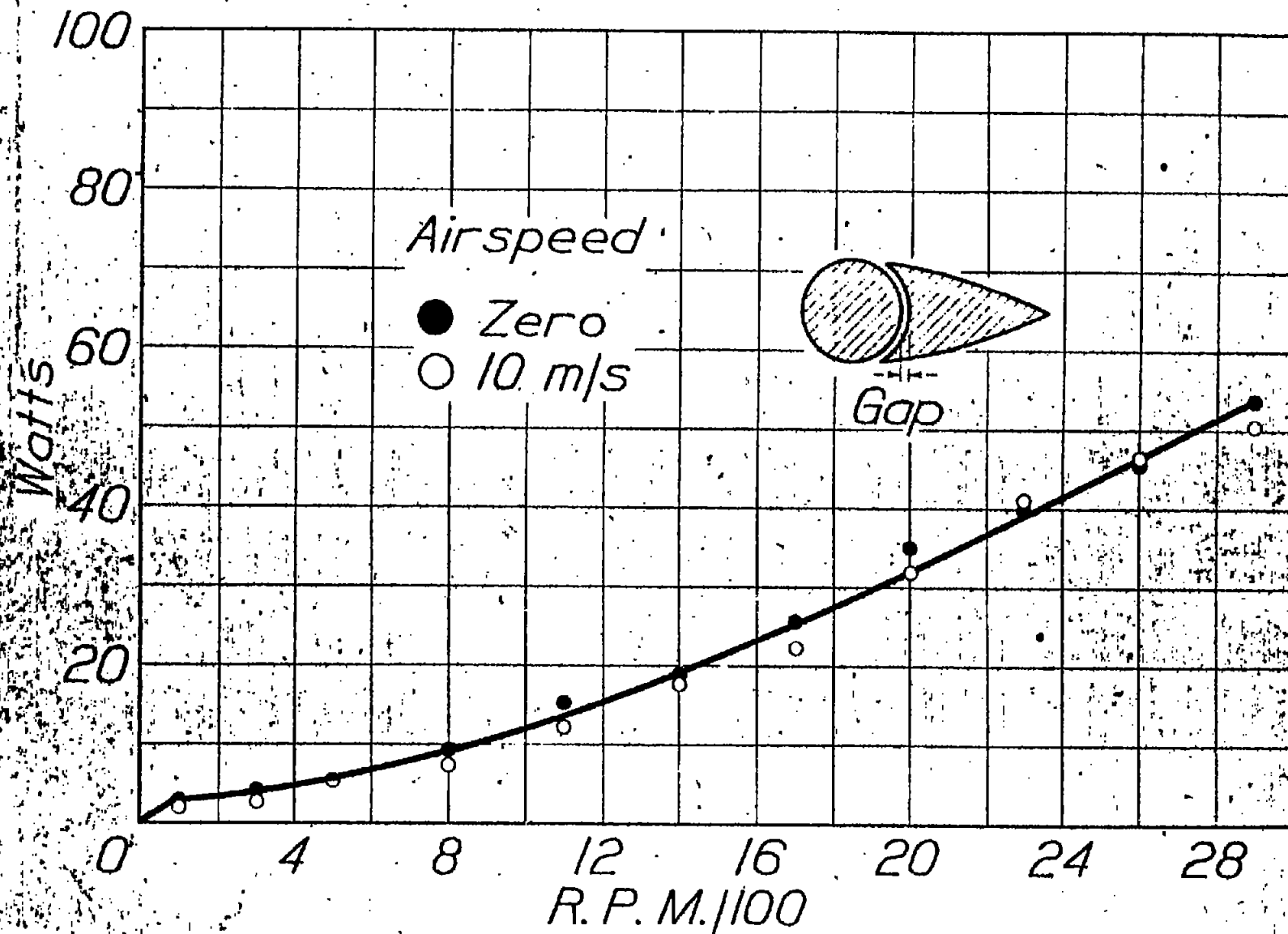


Fig. 12. Power consumption of combination strut.
Gap: $\frac{1}{8}$ "